NACA

RESEARCH MEMORANDUM

ALTITUDE-WIND-TUNNEL INVESTIGATION OF TAIL-PIPE BURNING WITH A WESTINGHOUSE X24C-4B AXIAL-FLOW TURBOJET ENGINE

By William A. Fleming and Lewis E. Wallner

Lewis Flight Propulsion Laboratory
Cleveland, Ohio

CLASSIFIED DOCUMENT

This document contains classified information affecting the National Defense of the United States within the meaning of the Espionage Act, USC 50:31 and 32. Its transmission or the revelation of its contents in any manner to an unauthorized person is prohibited by law. Information so classified may be imparted only to persons in the military and naval services of the United States, appropriate civilian officers and employees of the Federal Government who have a legitimate interest therein, and to United States citizens of known loyalty and discretion who of necessity must be informed thereof.

NATIONAL ADVISORY COMMITTEE FOR AERONAUTICS

WASHINGTON

December 13, 1948

NATIONAL ADVISORY COMMITTEE FOR AERONAUTICS

RESEARCH MEMORANDUM

ALTITUDE-WIND-TUNNEL INVESTIGATION OF TAIL-PIPE BURNING WITH A WESTINGHOUSE X24C-4B AXIAL-FLOW TURBOJET ENGINE

By William A. Fleming and Lewis E. Wallner

SUMMARY

Thrust augmentation of an axial-flow type turbojet engine by burning fuel in the tail pipe has been investigated in the NACA Cleveland altitude wind tunnel. The performance was determined over a range of simulated flight conditions and tail-pipe fuel flows. The engine tail pipe was modified for the investigation to reduce the gas velocity at the inlet of the tail-pipe combustion chamber and to provide an adequate seat for the flame; four such modifications were investigated.

The highest net-thrust increase obtained in the investigation was 86 percent with a net thrust specific fuel consumption of 2.91 and a total fuel-air ratio of 0.0523. The highest combustion efficiencies obtained with the four configurations ranged from 0.71 to 0.96. With three of the tail-pipe burners, for which no external cooling was provided, the exhaust nozzle and the rear part of the burner section were bright red during operation at high tail-pipe fuel-air ratios. With the tail-pipe burner for which fuel and water cooling were provided, the outer shell of the tail-pipe burner showed no evidence of elevated temperatures at any operating condition.

INTRODUCTION

Thrust augmentation of turbojet engines is of importance in increasing their usefulness and range of application. Utilization of the tail pipe for burning fuel provides a practical cycle for increasing the thrust of turbojet engines. This thrust increase is obtained without increasing the maximum temperature or stresses in the turbine buckets or otherwise disturbing the normal cycle of engine operation, provided that the tail-pipe nozzle area is

increased. A variable-area exhaust nozzle is therefore required to obtain maximum thrust both with and without tail-pipe burning.

A broad research program on thrust augmentation is being conducted at the NACA Lewis laboratory. As part of this program, an investigation of thrust augmentation by means of tail-pipe burning was conducted in the NACA Lewis altitude wind tunnel from May to August 1947 to study several tail-pipe-burner configurations on an axial-flow-compressor type turbojet engine with a thrust rating of 3000 pounds. Tail-pipe-burning results obtained on another axial-flow-compressor type turbojet engine in the altitude wind tunnel are reported in references 1 and 2 and results obtained at static sea-level conditions are presented in reference 3.

Operational and performance characteristics of four tail-pipe burner configurations were obtained over a range of simulated altitudes, flight Mach numbers, and tail-pipe fuel flows. Performance obtained with these tail-pipe burners is presented in both graphical and tabular form and compared with the performance of the engines in the normal configuration. The operational characteristics of each tail-pipe burner are discussed and the combustion efficiencies are presented.

INSTALLATION

Engine and Installation

Tail-pipe-burner performance was investigated with an early experimental Westinghouse 24C turbojet engine, which has an 11-stage axial-flow compressor, a double-annulus combustion chamber, and a two-stage turbine. Rated thrust of the engine is 3000 pounds at static sea-level conditions and an engine speed of 12,500 rpm. The engine air flow at this condition is approximately 58.5 pounds per second. The first two tail-pipe-burner configurations (A and B) were investigated on a standard engine and the other two configurations (C and D) were investigated on a modified engine having a slightly higher thrust and turbine-outlet temperature. The two engines are described and their performance is compared in reference 4. For the entire investigation, aviation gasoline that conformed to specifications AN-F-28, Amendment 3 and had a lower heating value of 19,300 Btu per pound was used in both the engines and the tail-pipe burners.

The engine was mounted in a wing nacelle installed in the 20-foot-diameter test section of the altitude wind tunnel, as shown

in figure 1. In order to simplify the installation, no cowling was installed around the engine. Dry refrigerated air was supplied to the engine through a duct from the tunnel make-up air system. This duct was connected to the engine-inlet duct by means of a slip joint with a labyrinth seal so that thrust and drag could be measured by scales. The air was throttled from approximately sea-level pressure to the desired pressure at the engine inlet while the required altitude pressure was maintained in the wind-tunnel test section.

Tail-Pipe Burners

Four tail-pipe-burner configurations were investigated in which the tail pipe was modified in order to reduce the tail-pipe gas velocity and to provide an adequate seat for the flame. Configurations A, B, and C consisted of three fuel-system and flame-holder installations mounted in a tail pipe having an inside diameter of $25\frac{3}{4}$ inches (fig. 2). Configuration A, with a slightly different diffuser section, has been investigated on another turbojet engine at static sea-level conditions (reference 3). Configuration D consisted of a tapered tail pipe, a fuel system, and a flame holder as an integral unit (fig. 3). This burner had a maximum inside diameter of $25\frac{1}{4}$ inches.

Configuration A. - A cross section of configuration A is shown in figure 4. The $25\frac{3}{4}$-inch-diameter burner section consisted of a cylinder 72 inches long, which was attached to the engine by an annular diffuser 22 inches long with an outlet-to-inlet area ratio of 2.43. A fixed-area conical nozzle 24 inches long having an outlet area of 298 square inches was installed on the tail pipe. No external cooling for the shell of the $25\frac{3}{4}$-inch-diameter tail pipe was provided except by the low-velocity air flowing through the wind-tunnel test section. Two quartz windows (fig. 2) were installed in the burner shell, one window immediately ahead of the flame holder and one immediately behind it, for observation of burning at the end of the diffuser cone and at the flame holder.

Fuel was injected into the burner through two rings of spray nozzles. The upstream ring consisted of 12 nozzles, which were rated at 40 gallons per hour at a differential pressure of 100 pounds per square inch and were installed in the inner cone of the diffuser section $9\frac{1}{2}$ inches downstream of the turbine flange. These nozzles injected fuel normal to the direction of gas flow. The downstream ring consisted of eighteen 30-gallon-per-hour nozzles mounted

with the tips of the nozzles $9\frac{3}{4}$ inches downstream of the front flange of the burner section. These nozzles were mounted in a $14\frac{1}{2}$-inch-diameter ring and injected fuel downstream. The blunt end of the diffuser inner cone provided a seat for the flame resulting from burning of the fuel injected through the upstream ring. For the data obtained with configuration A, approximately 25 percent of the tail-pipe fuel was injected through the upstream ring of nozzles and 75 percent through the downstream ring. A 2-inch-wide, semitoroidal flame holder (fig. 5) having a mean diameter of 16 inches was installed 9 inches behind the downstream fuel ring. The blocking area of this flame holder was 19 percent of the burner cross-sectional area. A small ignition pilot comprising a spark plug, a fuel nozzle, and a flame holder was installed immediately upstream of the flame holder to ignite the fuel in the tail pipe.

Configuration B. - Configuration B comprised the same tail pipe and fuel system as configuration A. For the data obtained with this configuration, approximately 20 percent of the tail-pipe fuel was injected through the upstream ring of nozzles and 80 percent through the downstream ring. In order to raise the combustion efficiency and the altitude limits of the tail-pipe burner, a flame holder having two annular V-type gutters (fig. 6) was installed in place of the semitoroidal flame holder. The mean diameters of the outer and inner gutters were 17 and 10 inches, respectively. The included angle of the gutters was 30° and the distance across the open end of the gutters was $1\frac{3}{4}$ inches. This flame holder blocked 32 percent of the burner cross-sectional area.

Configuration C. - Configuration C comprised the $25\frac{3}{4}$-inch-diameter tail pipe and the same flame holder used in configuration B. The downstream ring of fuel nozzles was removed and the upstream ring of nozzles was not used. A set of eight impinging jet spray bars (fig. 7) was installed in the diffuser section $4\frac{1}{2}$ inches downstream of the turbine flange. Fuel was injected through these spray bars in a downstream direction. The spray bars provided the possibility of obtaining a more homogeneous fuel mixture than the nozzles previously used. They could be easily made and modified without machining operations and could be installed without internal piping. The ignition system used with configuration C was the same as that used with configurations A and B.

Configuration D. - A cross section of configuration D is presented in figure 8. The burner section used was $37\frac{1}{4}$ inches long, circular in cross section, and tapered from a $25\frac{1}{4}$-inch inside diameter

at the upstream end to a 21-inch inside diameter at the downstream end. Immediately upstream of the burner section was a diffuser $33\frac{3}{8}$ inches long, which fastened to the $7\frac{1}{4}$-inch-long standard-engine tail-cone section. The ratio of burner-inlet area to turbine-outlet area is 2.35. A variable-area exhaust nozzle was used, which was designed to be closed for engine operation without tail-pipe burning and open with tail-pipe burning. With the nozzle in the open position, the area at the outlet was 273 square inches. All data, both with and without tail-pipe burning, were obtained with the nozzle in the open position. Fuel was passed rearward through helical passages welded to the shell of the burner to provide cooling for the shell and to preheat the fuel. Water was passed through a jacket welded around the fixed part of the tail-pipe nozzle to provide cooling. The movable part of the nozzle moved out of the flame when fuel was being burned in the tail pipe and thus required no cooling.

The flame holder used in configuration D included the fuel-injection system (fig. 9). The flame holder was mounted immediately behind the upstream flange of the tail-pipe burner section. Fuel was carried from the cooling passage at the rear of the burner forward to the center of the flame holder through six struts. The fuel-preheating system was designed to vaporize the fuel by the time it reached the flame holder. The preheated or vaporized fuel passed from the center of the flame holder through radial tubes and was injected in an upstream direction through a number of orifices approximately 1/4 inch in diameter. The flame holder had 12 radial fuel tubes 1/2 inch in diameter that extended from the center of the burner to the wall. Approximately $8\frac{1}{2}$ inches from the center of the flame holder, a circumferential fuel tube intersected the radial fuel tubes. Two circular metal strips 3/4 inch wide were welded to the downstream side of the radial tubes at mean diameters of $5\frac{1}{4}$ and $9\frac{3}{4}$ inches.

Instrumentation

A survey rake was mounted in the inlet duct ahead of the engine to measure the engine air flow. Pressure and temperature instrumentation was installed at eight stations throughout the engine and the tail-pipe burners. In order to prevent overheating, the airfoil section and the pressure tubes in the exhaust-nozzle-outlet survey rake were water-cooled.

PROCEDURE

Prior to operation with tail-pipe burning, performance data were obtained for the original engine with an exhaust-nozzle-outlet area of 183 square inches and for the modified engine with an exhaust-nozzle-outlet area of 171 square inches. These nozzles were selected to give rated engine performance at static sea-level conditions. Data thus obtained were used to provide a basis for evaluating the changes in performance resulting from the use of the various tail-pipe burners.

The range of simulated altitudes and simulated flight Mach numbers over which each configuration was investigated is shown in the following table:

Altitude (ft)	Flight Mach number			
	Configuration			
	A	B	C	D
5,000	0.264	0.275	0.258	0.171
15,000	-----	-----	-----	.531
25,000	.265	.272	.258	.727
25,000	.736	.537	.525	.863
25,000	.989	.727	.722	.977
25,000	-----	.869	-----	-----
25,000	-----	.984	-----	-----
30,000	-----	.509	-----	-----
35,000	.528	.491	-----	-----
40,000	-----	.509	-----	-----

At each simulated flight condition, the engine was operated at rated speed (12,500 rpm) and data were obtained at various fuel flows throughout the operable range of the tail-pipe burners. In most cases the minimum fuel flow was determined by combustion blow-out and the maximum fuel flow by limiting turbine-outlet temperature.

The limiting turbine-outlet temperature with and without tail-pipe burning was 1710° R for the original engine and 1860° R for the modified engine, as observed on the highest reading thermocouple. These conditions correspond to average turbine-outlet temperatures of about 1525° and 1650° R, respectively.

The total pressure at the compressor inlet was regulated to the value corresponding to the simulated flight Mach number. Complete free-stream ram-pressure recovery was assumed at the compressor inlet.

Air supplied to the engine was refrigerated to approximate the NACA standard temperature corresponding to the simulated flight condition. No inlet-air temperatures below about -20° F, corresponding to flight at high altitude and low flight Mach numbers, were obtained.

Thrust was determined from the balance scales and also from measurements obtained with the exhaust-nozzle survey rake. Only the rake thrust is used in the tabular and graphical presentations of the data because the survey-rake drag, which was not measured, affected the scale thrust and made the scale measurements less consistent than the rake measurements. Use of the rake thrust gives performance with 100-percent exhaust-nozzle expansion efficiency. Methods of calculating thrust, air flow, exhaust-gas temperature, and combustion efficiency are presented in the appendix. The symbols used in the calculations are also defined in the appendix.

RESULTS AND DISCUSSION

Performance

Data obtained with each of the four burner configurations are presented in table I. The combustion efficiency for each of the configurations is presented in figure 10 as a function of tail-pipe fuel-air ratio for a range of altitudes and flight Mach numbers. The tail-pipe fuel-air ratio is defined as the ratio of the tail-pipe fuel flow to the unburned air entering the tail-pipe burner, assuming complete combustion within the engine. Altitude and flight Mach number had no appreciable effect on the combustion efficiency at a given tail-pipe fuel-air ratio. Maximum combustion efficiencies obtained were 0.71 for configuration A, 0.76 for configuration B, and 0.96 for configuration C (figs. 10(a), 10(b), and 10(c)). These maximum efficiencies were obtained at tail-pipe fuel-air ratios between 0.02 and 0.03. Because of the poor fuel distribution in the tail-pipe burner, further increases in tail-pipe fuel-air ratio probably resulted in local fuel-air ratios greater than stoichiometric and therefore decreased combustion efficiencies.

Increasing the tail-pipe fuel-air ratio with configuration D raised the combustion efficiency for the range of data obtained. The highest combustion efficiency obtained with this configuration was 0.78 at a fuel-air ratio of 0.046. The data indicate that higher efficiencies might be obtained with configuration D if the exhaust-nozzle-outlet area were increased to permit operation at

higher fuel-air ratios without exceeding the temperature limits. Improved vaporization of the fuel as the tail-pipe fuel flow was increased probably accounts for the increase in combustion efficiency as the fuel-air ratio was increased, for the range of data obtained. A more homogeneous mixture of fuel and air in the tail pipe was probably obtained with configuration D than with the other configurations because peak combustion efficiency occurred at a higher tail-pipe fuel-air ratio.

A typical set of performance data is plotted in figure 11 for configuration B. In this figure are presented (a) net thrust, (b) engine fuel flow, (c) specific fuel consumption based on net thrust and total fuel flow, (d) total fuel-air ratio, (e) turbine-outlet total temperature, and (f) exhaust-gas total temperature as functions of the tail-pipe fuel flow with a fixed-area exhaust nozzle. Significant results of this investigation were obtained at conditions where limiting turbine-outlet temperatures were reached; therefore, the points representing limiting turbine-outlet temperature at each flight Mach number are joined by a dashed curve in figure 11. The succeeding discussion of each burner configuration is confined to the results obtained at limiting turbine-outlet temperature, as determined from curves similar to figure 11.

The engine performance with tail-pipe burning is presented in figures 12 to 16 for configurations B, C, and D. Engine performance with the standard tail pipe and exhaust nozzle is also presented in these figures. Because data with configuration A were obtained only below the limiting turbine-outlet temperature, they are included only in tabular form. Absolute values of performance with configuration B cannot be compared directly with those of configurations C and D because of the differences between the original and modified engines. Inasmuch as the data were obtained with the same engine, performance for configurations C and D is compared, although the exhaust-nozzle-outlet areas were different.

The maximum exhaust-gas total temperature (3470° R), at limiting turbine-outlet temperature, was obtained with configuration C at a flight Mach number of 0.72 (fig. 12(b)). This temperature corresponds to a tail-pipe temperature ratio of 2.1 and a tail-pipe temperature rise of 1820° R. Values of exhaust-gas temperature are presented in figure 12(a) for configuration B and in figure 12(b) for configurations C and D. A part of the thrust augmentation that is obtained at flight Mach numbers above 0.55 is due to the higher turbine-outlet temperatures that can be maintained with the modified tail pipe and tail-pipe burning, as compared with the engine equipped with the standard tail pipe and a fixed-area exhaust nozzle.

The values of net thrust (fig. 13), increase in net thrust (fig. 14), specific fuel consumption based on net thrust and total fuel flow (fig. 15), total fuel-air ratio (fig. 16), and exhaust-gas total temperature (fig. 12) at the minimum and maximum flight Mach numbers investigated at an altitude of 25,000 feet are presented in the following table for configurations B, C, and D:

Configuration	Flight Mach number	Net thrust (lb)	Increase in net thrust (percent)	Specific fuel consumption based on net thrust and total fuel flow (lb/(hr)(lb thrust))	Total fuel-air ratio	Exhaust-gas total temperature (°R)
B	0.272	1480	22	2.54	0.0415	2660
	.984	2780	86	2.91	.0523	2780
C	0.258	1730	31	2.57	0.0520	3330
	.722	2595	73	2.55	.0565	3470
D	0.727	2320	55	2.45	0.0500	2940
	.977	2920	79	2.36	.0475	2960

The exhaust-gas total temperature increased slightly with flight Mach number for each configuration. As would be expected, however, the net thrust increased rapidly with flight Mach number. The trend of the net thrust specific fuel consumption was similar to that of the total fuel-air ratio as the flight Mach number was varied. A limitation was imposed on the performance by the exhaust nozzles. A slight increase in exhaust-nozzle-outlet area would have made it possible to increase the total fuel-air ratio to a value closer to a stoichiometric mixture, without increasing the turbine-outlet temperature, and thereby obtain the maximum net thrust.

At limiting turbine-outlet temperatures, the increase in jet thrust and tail-pipe total-temperature ratio obtained with tail-pipe burning are approximately proportional to the ratio of exhaust-nozzle-outlet area with tail-pipe burning to exhaust-nozzle-outlet area without tail-pipe burning (reference 1). It follows that the increase in net thrust would also be greater for higher exhaust-nozzle-outlet-area ratios. Because the ratio of exhaust-nozzle-outlet area with and without tail-pipe burning for configuration C (1.74) was greater than that with configuration B (1.63), the increase in net thrust and the tail-pipe total-temperature ratio were also greater for configuration C. The increase in net thrust and the tail-pipe total-temperature ratio at a given flight condition were lower for configuration D than for configuration C because the ratio of exhaust-nozzle-outlet area with and without tail-pipe burning was less for configuration D.

Operational Characteristics

Configuration A. - The highest thrust and the smoothest burner operation, without overheating the burner shell, were obtained with configuration A when approximately 75 percent of the tail-pipe fuel was injected through the downstream ring of nozzles and 25 percent through the nozzles in the inner cone of the diffuser section. Increasing the percentage of fuel injected through the nozzles in the diffuser section overheated the tail-pipe burner shell and resulted in rough burning accompanied by heavy pulsations or combustion blow-out. The maximum altitude at which the burner operated was 39,000 feet at a flight Mach number of about 0.50, at which combustion blow-out occurred several times. Between altitudes of 30,000 and 39,000 feet, the flame seated on the end of the diffuser inner cone became quite unstable and flickered constantly. Because operation of the ignition pilot was unsatisfactory, the tail-pipe fuel was ignited by accelerating the engine rapidly from about 6000 rpm. Satisfactory starts were thus made at altitudes up to 30,000 feet, but above this altitude combustion blow-out occurred during the acceleration in either the engine or the tail-pipe burner after the tail-pipe fuel ignited.

Configuration B. - The highest thrust and the smoothest burner operation, without overheating the burner shell, were obtained with configuration B, when 80 percent of the fuel was injected through the downstream ring of nozzles and 20 percent through the nozzles in the diffuser inner cone. Raising the percentage of fuel flow injected through the nozzles in the diffuser cone overheated the burner shell and resulted in rough burning. Stable burner operation was obtained with all the fuel injected through the downstream ring of fuel nozzles; however, the thrust was not so high as that obtained with 80 percent of the fuel injected through the downstream nozzles. The maximum operating altitude with this burner was 44,000 feet at a flight Mach number of about 0.50, at which combustion blow-out occurred. The starting characteristics and the method of igniting the tail-pipe fuel were the same with this burner as with configuration A.

Configuration C. - Initial operation with configuration C indicated that the shell of the tail-pipe burner became excessively hot at high fuel-air ratios. In order to decrease the amount of burning near the shell of the burner, the jets in the impinging jet spray bars were relocated in order to concentrate most of the fuel in the inner part of the diffuser passage. After this modification was made, the shell operated somewhat cooler, but it still became too hot for a satisfactory flight installation. All data presented in this report for configuration C were obtained with the final spray-bar modification shown in figure 7. No maximum operating

altitude was obtained for this configuration. The starting characteristics and the method of igniting the tail-pipe fuel were the same for this burner as for configurations A and B; however, no data were obtained above an altitude of 25,000 feet. Near the end of this part of the investigation, a large section of the flame holder was burned away, which was probably caused by burning ahead of the flame holder in the diffuser section. Installing the impinging jet spray bars further downstream in the diffuser would probably improve tail-pipe shell cooling and lengthen the flame-holder life.

Configuration D. - Burning was somewhat smoother with configuration D than with the other three configurations, as indicated by the reduction in rumble or pulsation that is usually present with tail-pipe burning. The fuel in this burner was also ignited by accelerating the engine, inasmuch as the ignition pilot did not operate at altitude. It was very difficult, however, to ignite the burner fuel in this manner at altitudes above 20,000 feet. The temperature rise of the fuel in passing through the shell of this tail-pipe burner was usually between 110° and 165° F. No data were obtained with this configuration at altitudes above 25,000 feet.

Shell cooling. - With configurations A, B, and C, the shell of the exhaust nozzle and the rear part of the burner section were bright red during operation at high tail-pipe fuel-air ratios. The shell temperature, as estimated by the metal color, was about the same with configurations A and B; however, with configuration C the shell became somewhat hotter and a slightly greater part of the burner section became red. Either redistribution of the tail-pipe fuel or external cooling or both would be required to cool these configurations satisfactorily for flight use. With the fuel and water cooling of the shell provided for configuration D, the outer shell of the tail-pipe burner showed no evidence of elevated temperatures at any operating condition. Some difficulty was encountered, however, with leaks on the outside of the burner section at the welds of the fuel passages due to differential expansion of the inner and outer shell.

Ignition pilots. - A definite need is indicated for a tail-pipe-burner ignition pilot that will operate at maximum engine speed and at high altitudes. Accelerating the engine from a low speed is an unsatisfactory method of igniting the tail-pipe fuel because of the loss in thrust during the starting period, possible combustion blowout in the engine at high altitudes, and the high temperatures imposed on the turbine. A number of variations of the type of ignition pilot indicated in figures 5, 6, and 9 were used but none of them operated at high altitudes and most of them did not operate at

high engine speeds. Two considerations were found to be of greatest importance; one was a dependable spark plug for ignition of the pilot fuel and the other was proper metering of the pilot fuel.

SUMMARY OF RESULTS

The following results were obtained from an investigation of an axial-flow-compressor-type turbojet engine in the NACA Cleveland altitude wind tunnel over a range of simulated flight conditions with four tail-pipe-burner configurations:

1. The highest net-thrust increase obtained in the investigation was 86 percent at an altitude of 25,000 feet and a flight Mach number of 0.984. The corresponding net thrust specific fuel consumption was 2.91 and the total fuel-air ratio was 0.0523.

2. The highest combustion efficiencies obtained with the four configurations ranged from 0.71 to 0.96.

3. Maximum operable altitudes for two tail-pipe-burner configurations were 39,000 and 44,000 feet at a flight Mach number of approximately 0.50.

4. The highest exhaust-gas total temperature obtained in the investigation at limiting turbine-outlet temperature was 3470° R, which corresponds to a tail-pipe total-temperature ratio of 2.1.

5. With three of the configurations, for which no external cooling of the tail-pipe-burner shell was provided, the exhaust nozzle and the rear part of the burner section were bright red during operation at high tail-pipe fuel-air ratios. With the tail-pipe burner for which fuel and water cooling were provided, the outer shell of the tail-pipe burner showed no evidence of elevated temperatures at any operating condition.

Lewis Flight Propulsion Laboratory,
National Advisory Committee for Aeronautics,
Cleveland, Ohio.

APPENDIX - METHODS OF CALCULATION

Symbols

The following symbols are used in the calculations:

A	cross-sectional area, sq ft
c_p	specific heat of gas at constant pressure, Btu/(lb)(°R)
F_j	jet thrust, lb
F_n	net thrust, lb
g	acceleration due to gravity, 32.2 ft/sec^2
h	enthalpy, Btu/lb
h_c	heating value of fuel, Btu/lb
J	mechanical equivalent of heat, 778 ft-lb/Btu
M	Mach number
P	total pressure, lb/sq ft absolute
p	static pressure, lb/sq ft absolute
R	gas constant, 53.4 ft-lb/(lb)(°R)
T	total temperature, °R
T_i	indicated temperature, °R
t	static temperature, °R
V	velocity, ft/sec
W_a	air flow, lb/sec
W_f	fuel flow, lb/hr
W_g	gas flow, lb/sec
W_f/F_n	specific fuel consumption based on net thrust and total fuel flow, lb/(hr)(lb thrust)

f/a total fuel-air ratio

γ ratio of specific heats for gases

η efficiency

τ total-temperature ratio across tail-pipe burner, T_8/T_7

Subscripts:

b burner

e engine

f fuel

t tail-pipe burner

0 tunnel test-section free-air stream

1 inlet duct

2 compressor inlet

7 tail-pipe-burner inlet

8 exhaust-nozzle outlet

Calculations

Temperature. - By use of an experimentally determined impact recovery factor of 0.85, static temperature was determined from indicated temperature by applying the factor to the adiabatic relation between the temperature and the pressure in the following manner:

$$t = \frac{T_i}{1 + 0.85\left[\left(\frac{p}{p}\right)^{\frac{\gamma-1}{\gamma}} - 1\right]} \qquad (1)$$

Air flow. - The air flow through the engine was determined from pressure and temperature measurements obtained with a vertical survey rake installed in the engine inlet duct (station 1). Air flow was calculated by the equation

$$W_a = \frac{p_1 A_1}{R} \sqrt{\frac{2Jgc_p}{t_1} \left[\left(\frac{P_1}{p_1} \right)^{\frac{\gamma_1 - 1}{\gamma_1}} - 1 \right]} \qquad (2)$$

The static temperature in equation (2) was obtained by use of equation (1).

Jet thrust. - Jet thrust was calculated from pressure measurements at the exhaust-nozzle outlet by the equation

$$F_j = \frac{2\gamma_8 p_8 A_8}{\gamma_8 - 1} \left[\left(\frac{P_8}{p_8} \right)^{\frac{\gamma_8 - 1}{\gamma_8}} - 1 \right] + A_8(p_8 - p_0) \qquad (3)$$

The assumptions involved in using this equation are that there is no total-pressure loss across the exhaust nozzle and that there is complete adiabatic expansion of the jet from the nozzle outlet to ambient conditions. Use of equation (3) gives results for a nozzle efficiency of 100 percent.

Equivalent airspeed. - Inasmuch as all calculations are based on 100-percent ram-pressure recovery at the compressor inlet (station 2) the equivalent airspeed corresponding to the ram-pressure ratio at the engine inlet can be expressed by

$$V_0 = \sqrt{2Jgc_p T_{i,2} \left[1 - \left(\frac{p_0}{P_2} \right)^{\frac{\gamma_2 - 1}{\gamma_2}} \right]} \qquad (4)$$

The equivalent free-stream total temperature was assumed equal to the compressor-inlet indicated temperature. The use of this assumption introduces an error in airspeed of less than 1 percent.

Net thrust. - The equivalent free-stream momentum of the inlet air was subtracted from the jet thrust by combining equations (2), (3), and (4) in the following expression for net thrust:

$$F_n = F_j - \frac{W_a V_0}{g} \tag{5}$$

Exhaust-gas total temperature. - The exhaust-gas total temperature was calculated from the tail-pipe-rake jet thrust and the mass gas flow through the tail-pipe burner. This equation is based on the assumption that there is adiabatic expansion from the nozzle outlet to ambient pressure. This assumption involves an error of less than 1 percent.

$$T_8 = \frac{(\gamma_8 - 1)\, g (F_j)^2}{2\gamma_8 R (W_{g,8})^2 \left[1 - \left(\frac{p_0}{p_8} \right)^{\frac{\gamma_8 - 1}{\gamma_8}} \right]} \tag{6}$$

Combustion efficiency. - The tail-pipe combustion efficiency was obtained by dividing the heat added in the tail pipe by the heat content of the fuel supplied, disregarding dissociation of the exhaust gases.

$$\eta_{b,t} = \frac{3600\, W_{g,8}\, h_8 - 3600\, W_{g,7}\, h_7 - W_{f,t}\, h_{f,t}}{h_{c,t}\, W_{f,t}} \tag{7}$$

The numerator of the right-hand side of this equation is composed of the total heat in the gas leaving the tail pipe, the total heat in the gas entering the tail pipe, and the initial heat in the liquid fuel added in the tail pipe.

Tail-pipe fuel-air ratio. - The tail-pipe fuel-air ratio is defined as the ratio of the tail-pipe fuel flow to the unburned air entering the tail-pipe burner. The assumption used in obtaining this equation is that the fuel injected into the engine combustion chamber is completely burned. Combining the air flow, the engine fuel flow, and the tail-pipe fuel flow gives the following equation for tail-pipe fuel-air ratio:

$$(f/a)_t = \frac{W_{f,t}}{3600\ W_a - \frac{W_{f,e}}{0.067}} \qquad (8)$$

The value of 0.067 in the denominator is the stoichiometric fuel-air ratio for the fuel used.

REFERENCES

1. Fleming, W. A., and Dietz, R. O.: Altitude-Wind-Tunnel Investigations of Thrust Augmentation of a Turbojet Engine. I - Performance with Tail-Pipe Burning. NACA RM No. E6I20, 1946.

2. Fleming, William A., and Golladay, Richard L.: Altitude-Wind-Tunnel Investigation of Thrust Augmentation of a Turbojet Engine. III - Performance with Tail-Pipe Burning in Standard-Size Tail Pipe. NACA RM No. E7F10, 1947.

3. Lundin, Bruce T., Dowman, Harry W., and Gabriel, David S.: Experimental Investigation of Thrust Augmentation of a Turbojet Engine at Zero Ram by Means of Tail-Pipe Burning. NACA RM No. E6J21, 1947.

4. Meyer, Carl L., and Bloomer, Harry E.: Altitude-Wind-Tunnel Investigation of Performance and Windmilling Drag Characteristics of Westinghouse X24C-4B Axial-Flow Turbojet Engine. NACA RM No. E8J25a, 1948.

TABLE I. - PERFORMANCE DATA

	1	2	3	4	5	6	7	8	9	10	11
Run	Altitude (ft)	Flight Mach number M_0	Ambient pressure p_0 (lb/sq ft abs.)	Compressor-inlet total pressure $P_{2,2}$ (lb/sq ft abs.)	Compressor-inlet-indicated temperature $T_{i,2}$ (°R)	Engine fuel flow $W_{f,e}$ (lb/hr)	Tail-pipe fuel flow $W_{f,t}$ (lb/hr)	Total fuel flow W_f (lb/hr)	Jet thrust F_j (lb)	Net thrust F_n (lb)	Air flow W_a (lb/sec)
Configuration A											
1	5,000	0.265	1752	1840	508	1626	0	1626	1433	961	52.03
2	5,000	.263	1752	1837	508	1871	2640	4511	2357	1892	51.88
3	5,000	.272	1752	1838	510	1980	3520	5500	2599	2135	51.61
4	5,000	.255	1752	1833	510	2060	4180	6240	2752	2302	51.59
5	25,000	.263	781	816	449	907	0	907	757	547	24.91
6	25,000	.263	781	816	447	1149	1890	3039	1499	1290	24.89
7	25,000	.268	781	818	450	1169	2150	3319	1544	1331	24.80
8	25,000	.266	781	817	448	1200	2420	3620	1608	1396	24.88
9	25,000	.263	781	816	443	1239	2680	3919	1675	1465	25.03
10	25,000	.983	781	1447	515	1200	0	1200	1730	464	40.67
11	25,000	.991	781	1461	498	1471	2720	4191	3044	1748	42.06
12	25,000	.994	778	1466	502	1705	3700	5405	3597	2293	41.96
13	25,000	.989	778	1453	499	1881	4880	6761	3953	2669	41.67
14	35,000	.521	498	599	434	715	0	715	638	337	18.65
15	35,000	.528	498	602	460	897	1600	2497	1324	1021	18.01
Configuration B											
1	5,000	0.275	1760	1855	510	1626	0	1626	1439	943	52.66
2	5,000	.265	1753	1840	517	1685	1610	3295	1790	1322	51.21
3	5,000	.273	1746	1839	517	1862	1910	3772	2154	1674	51.08
4	5,000	.276	1753	1847	515	2304	3160	5464	2647	2159	51.55
5	5,000	.273	1760	1853	513	2325	4600	6925	3056	2569	52.11
6	5,000	.286	1753	1838	509	2485	6050	8535	3319	2860	51.74
7	25,000	.271	781	822	445	917	0	917	767	548	25,31
8	25,000	.273	774	815	454	977	1040	2017	1119	899	24.96
9	25,000	.260	785	823	453	1058	1360	2418	1277	1068	24.98
10	25,000	.276	778	820	454	1099	1500	2599	1371	1148	25.04
11	25,000	.280	774	817	455	1129	1990	3119	1558	1333	24.88
12	25,000	.276	785	827	450	1297	2600	3897	1716	1494	25.11
13	25,000	.269	778	818	455	1297	2720	4017	1755	1539	24.97
14	25,000	.515	781	936	462	957	0	957	940	475	28.28
15	25,000	.523	774	933	467	1018	1215	2233	1348	874	28.24
16	25,000	.532	788	955	465	1200	1900	3100	1740	1251	28.74
17	25,000	.543	774	946	462	1355	2900	4255	2080	1590	28.33
18	25,000	.549	774	950	459	1472	3890	5362	2275	1776	28.67
19	25,000	.729	781	1113	481	1038	0	1038	1249	489	32.74
20	25,000	.730	781	1114	473	1118	1420	2538	1726	964	33.08
21	25,000	.719	796	1123	472	1491	2990	4481	2564	1800	34.07
22	25,000	.732	774	1105	473	1626	4450	6076	2799	2045	33.13
23	25,000	.723	774	1100	479	1706	5070	6776	2911	2159	32.66
24	25,000	.731	774	1104	475	1706	5200	6906	2952	2191	32.94
25	25,000	.722	785	1111	476	1726	5290	7016	2957	2201	33.07
26	25,000	.851	788	1264	496	1099	0	1099	1467	482	36.49
27	25,000	.866	781	1273	491	1200	1810	3010	2208	1201	36.90
28	25,000	.868	781	1275	490	1567	3240	4807	3005	1997	36.90
29	25,000	.869	774	1266	492	1724	4700	6424	3282	2275	36.76
30	25,000	.873	781	1283	490	1881	6120	8001	3563	2541	37.23
31	25,000	.976	788	1450	514	1200	0	1200	1746	475	41.07
32	25,000	.984	781	1449	504	1327	2150	3477	2779	1509	41.20
33	25,000	.987	781	1456	505	1665	3280	4945	3438	2164	41.13
34	25,000	.988	781	1459	505	1832	4620	6452	3780	2497	41.40
35	25,000	.985	774	1440	497	2000	5950	7950	4012	2744	41.36
36	30,000	.534	623	752	453	826	0	826	809	429	22.90
37	30,000	.509	627	748	453	1200	2980	4180	1790	1417	23.14
38	35,000	.537	493	600	455	695	0	695	654	344	18.24
39	35,000	.491	496	585	452	906	1890	2796	1295	1021	17.62
40	40,000	.534	387	470	462	595	0	595	524	285	14.04
41	40,000	.509	391	467	446	766	1210	1976	1021	778	15.19

WITH TAIL-PIPE BURNING

12	13	14	15	16	17	18	19	20	21	
Specific fuel consumption W_f/F_n (lb/(hr)(lb thrust))	Total fuel-air ratio f/a	Tail-pipe fuel-air ratio $(f/a)_t$	Tail-pipe combustion efficiency $\eta_{b,t}$	Turbine-outlet total pressure P_6 (lb/sq ft abs.)	Turbine-outlet static pressure p_6 (lb/sq ft abs.)	Turbine-outlet total temperature T_6, (°R)	Exhaust-nozzle total pressure P_8 (lb/sq ft abs.)	Exhaust-nozzle static pressure p_8 (lb/sq ft abs.)	Exhaust-gas total temperature T_8, (°R)	Run
Configuration A										
1.693	0.0087	-----	----	2321	1789	1163	2138	1795	----	1
2.384	.0242	0.0166	0.693	2564	2104	1277	2417	1855	1918	2
2.577	.0296	.0225	.679	2659	2210	1331	2496	1878	2137	3
2.710	.0336	.0270	.640	2723	2285	1370	2545	1895	2250	4
1.658	.0101	-----	----	1089	818	1182	984	802	----	5
2.356	.0339	.0261	.725	1328	1111	1418	1227	885	2363	6
2.493	.0372	.0300	.662	1356	1139	1455	1250	895	2408	7
2.593	.0404	.0338	.651	1377	1156	1470	1269	895	2512	8
2.675	.0435	.0374	.636	1398	1181	1486	1289	913	2597	9
2.586	.0082	-----	----	1660	487	1168	1312	907	----	10
2.398	.0277	.0210	.635	1989	1605	1253	1795	1173	1983	11
2.358	.0358	.0295	.711	2191	1827	1376	2002	1315	2428	12
2.533	.0451	.0400	.686	2321	1966	1467	2136	1395	2753	13
2.122	.0106	-----	----	798	509	1229	676	520	----	14
2.447	.0385	.0311	.777	993	829	1489	916	630	2652	15
Configuration B										
1.724	0.0086	-----	----	2342	1791	1157	2151	1812	----	1
2.492	.0179	0.0101	0.426	2417	1921	1208	2247	1826	1478	2
2.253	.0205	.0122	.710	2573	2112	1288	2358	1860	1779	3
2.531	.0294	.0209	.671	2764	2312	1376	2519	1901	2158	4
2.696	.0369	.0301	.674	2932	2495	1452	2661	1957	2444	5
2.984	.0458	.0405	.609	3026	2603	1508	2747	1986	2655	6
1.673	.0101	-----	----	1111	823	1199	989	805	----	7
2.244	.0224	.0139	.589	1194	952	1293	1096	832	1739	8
2.264	.0269	.0183	.677	1266	1036	1351	1161	862	2004	9
2.264	.0288	.0203	.728	1284	1057	1382	1182	860	2143	10
2.340	.0348	.0273	.772	1344	1127	1448	1243	885	2461	11
2.608	.0431	.0366	.680	1439	1228	1544	1312	930	2668	12
2.610	.0447	.0386	.687	1430	1215	1556	1318	927	2743	13
2.015	.0094	-----	----	1189	815	1156	1041	810	----	14
2.555	.0220	.0140	.548	1286	1004	1224	1172	857	1668	15
2.478	.0300	.0242	.715	1482	1207	1359	1320	924	2145	16
2.676	.0417	.0354	.676	1584	1336	1489	1434	986	2602	17
3.019	.0520	.0479	.582	1667	1432	1555	1505	1026	2773	18
2.123	.0088	-----	----	1342	761	1153	1140	838	----	19
2.633	.0213	.0139	.548	1468	1124	1198	1306	900	1632	20
2.489	.0370	.0302	.708	1816	1522	1412	1629	1090	2465	21
2.971	.0516	.0477	.585	1893	1617	1533	1700	1136	2766	22
3.140	.0576	.0550	.554	1921	1649	1580	1743	1167	2878	23
3.152	.0582	.0559	.545	1934	1658	1571	1762	1187	2868	24
3.188	.0589	.0567	.543	1967	1692	1583	1772	1190	2879	25
2.280	.0084	-----	----	1486	694	1146	1221	866	----	26
2.506	.0227	.0157	.620	1656	1277	1190	1482	790	1745	27
2.407	.0362	.0296	.732	1978	1665	1390	1783	1182	2476	28
2.824	.0485	.0440	.603	2090	1784	1486	1883	1251	2707	29
3.149	.0597	.0578	.544	2213	1904	1567	1996	1325	2894	30
2.526	.0081	-----	----	1625	617	1147	1319	915	----	31
2.304	.0234	.0167	.689	1887	1483	1205	1695	1112	1855	32
2.285	.0334	.0267	.755	2160	1805	1371	1948	1289	2395	33
2.584	.0433	.0380	.654	2308	1969	1466	2078	1378	2628	34
2.897	.0534	.0500	.563	2405	2065	1526	2166	1440	2772	35
1.925	.0100	-----	----	972	650	1202	850	656	----	36
2.950	.0502	.0456	.570	1326	1128	1549	1203	829	2693	37
2.020	.0106	-----	----	779	517	1233	676	519	----	38
2.738	.0441	.0380	.650	988	833	1476	905	626	2656	39
2.088	.0118	-----	----	620	407	1307	533	406	----	40
2.540	.0361	.0279	.562	782	645	1554	716	495	2245	41

TABLE I. - PERFORMANCE DATA WITH

Run	1 Altitude (ft)	2 Flight Mach number M_0	3 Ambient pressure p_0 (lb/sq ft abs.)	4 Compressor-inlet total pressure P_2, (lb/sq ft abs.)	5 Compressor-inlet-indicated temperature $T_{1,2}$, (°R)	6 Engine fuel flow $W_{f,e}$ (lb/hr)	7 Tail-pipe fuel flow $W_{f,t}$ (lb/hr)	8 Total fuel flow W_f (lb/hr)	9 Jet thrust F_j (lb)	10 Net thrust F_n (lb)	11 Air flow W_a (lb/sec)
Configuration C											
1	25,000	0.241	781	814	479	296	0	796	552	361	23.73
2	25,000	.261	774	812	478	947	1980	2927	1217	1012	23.76
3	25,000	.270	774	814	478	1317	3050	4367	1915	1700	23.99
4	25,000	.249	781	815	477	1414	3900	5314	2093	1898	23.66
5	25,000	.252	781	816	481	1433	4880	6313	2144	1946	23.62
6	25,000	.529	781	945	463	916	0	916	934	465	27.77
7	25,000	.523	774	933	465	1249	1900	3149	1914	1448	27.82
8	25,000	.527	774	935	463	1239	1900	3139	1922	1455	27.12
9	25,000	.528	781	944	466	1355	2200	3555	2101	1628	27.96
10	25,000	.525	781	942	464	1520	2880	4400	2377	1906	28.07
11	25,000	.524	781	942	462	1626	3640	5266	2608	2136	28.18
12	25,000	.525	774	934	460	1655	4320	5975	2680	2217	27.65
13	25,000	.725	778	1104	471	977	0	977	1171	420	32.89
14	25,000	.724	778	1103	469	1317	2410	3727	2478	1729	32.92
15	25,000	.722	781	1106	470	1636	3410	5046	3003	2256	32.85
16	25,000	.721	781	1104	470	1813	4550	6363	3295	2549	32.86
17	25,000	.682	838	1154	464	1970	5600	7570	3626	2872	34.74
18	25,000	.842	824	1309	455	2182	5020	7202	4231	3213	39.70
Configuration D											
1	5,000	0.169	1752	1787	510	1646	0	1646	1450	1161	49.86
2	5,000	.176	1752	1791	504	1960	3320	5280	2118	1816	50.18
3	5,000	.173	1752	1789	509	2081	3780	5861	2318	2023	49.67
4	5,000	.160	1746	1778	509	2233	4180	6413	2559	2287	49.67
5	5,000	.176	1739	1778	501	2386	4520	6906	2833	2530	50.62
6	15,000	.531	1189	1440	497	1258	0	1258	1321	597	41.23
7	15,000	.528	1189	1437	495	1549	3300	4849	2139	1428	40.74
8	15,000	.532	1189	1441	491	1734	3700	5434	2427	1708	41.08
9	15,000	.532	1190	1442	497	2060	4240	6300	2840	2119	40.99
10	15,000	.532	1186	1437	485	2335	4720	7055	3387	2669	41.29
11	25,000	.716	781	1099	482	988	0	988	1234	515	31.47
12	25,000	.725	778	1103	479	1259	2820	4079	2053	1310	32.33
13	25,000	.730	778	1109	473	1453	3240	4693	2363	1618	32.39
14	25,000	.723	778	1101	474	1636	3560	5196	2684	1944	32.44
15	25,000	.729	778	1107	472	1745	3800	5545	2728	1979	32.66
16	25,000	.728	778	1106	476	1921	3980	5901	3172	2439	31.86
17	25,000	.861	781	1267	498	1079	0	1078	1462	482	35.79
18	25,000	.864	781	1270	495	1317	3060	4377	2324	1338	36.06
19	25,000	.865	778	1267	492	1375	3180	4555	2410	1426	36.05
20	25,000	.863	783	1272	490	1443	3350	4793	2509	1519	36.43
21	25,000	.862	781	1268	490	1724	3760	5484	2919	1935	36.20
22	25,000	.863	784	1273	496	2142	4320	6462	3678	2682	36.45
23	25,000	.975	781	1438	503	1190	0	1190	1841	596	40.70
24	25,000	.980	778	1438	511	1404	3200	4604	2706	1463	40.15
25	25,000	.975	781	1434	510	1501	3400	4901	2826	1596	39.98
26	25,000	.976	778	1433	509	1501	3630	5131	2862	1633	39.93
27	25,000	.981	781	1445	510	1881	4100	5981	3475	2233	40.13
28	25,000	.975	781	1434	510	2020	4250	6270	3738	2508	39.97
29	25,000	.976	778	1432	516	2102	4460	6562	3884	2665	39.34
30	25,000	.961	800	1450	505	2284	4650	6934	4143	2910	40.67

[a]Data not obtained.

TAIL-PIPE BURNING - Concluded

12	13	14	15	16	17	18	19	20	21	
Specific fuel consumption W_f/F_n (lb/(hr) (lb thrust))	Total fuel-air ratio f/a	Tail-pipe fuel-air ratio $(f/a)_t$	Tail-pipe combustion efficiency $\eta_{b,t}$	Turbine-outlet total pressure P_6 (lb/sq ft abs.)	Turbine-outlet static pressure p_6 (lb/sq ft abs.)	Turbine-outlet total temperature T_6, (°R)	Exhaust-nozzle total pressure P_8 (lb/sq ft abs.)	Exhaust-nozzle static pressure p_8 (lb/sq ft abs.)	Exhaust-gas total temperature T_8, (°R)	Run
Configuration C										
2.207	0.0093	-----	----	1057	799	1131	954	788	----	1
2.892	.0342	.0277	.531	1212	1007	1263	1122	825	2084	2
2.569	.0506	.0457	.828	1480	1287	1634	1368	939	3251	3
2.800	.0624	.0609	.807	1567	1377	1725	1434	963	3666	4
3.244	.0742	.0768	.676	1577	1391	1735	1451	967	3704	5
1.970	.0092	-----	----	1155	804	1122	1034	795	----	6
2.175	.0314	.0234	.970	1489	1228	1271	1356	881	2555	7
2.157	.0315	.0233	.992	1487	1230	1380	1362	894	2574	8
2.184	.0353	.0274	.993	(a)	(a)	1457	1435	942	2799	9
2.308	.0435	.0367	.944	1690	1447	1588	1543	1027	3144	10
2.465	.0519	.0472	.902	1766	1526	1655	1623	1056	3451	11
2.695	.0600	.0582	.821	1784	1533	1665	1642	1055	3627	12
2.326	.0083	-----	----	1329	724	1107	1109	815	----	13
2.156	.0314	.0243	.898	1742	1473	1309	1579	1048	2463	14
2.237	.0427	.0363	.942	1939	1678	1505	1772	1138	3095	15
2.496	.0538	.0499	.838	2056	1798	1621	1884	1221	3404	16
3.100	.0605	.0586	.798	2248	1985	1708	2058	1349	3570	17
2.242	.0504	.0455	.919	2406	2093	1604	2272	1445	3410	18
Configuration D										
1.418	0.0092	-----	----	2432	1815	1191	2197	1850	----	1
2.907	.0292	0.0220	0.253	2723	2137	1296	2430	1935	1614	2
2.897	.0328	.0255	.312	2820	2268	1360	2512	1985	1784	3
2.804	.0359	.0288	.378	2950	2375	1428	2593	2020	1976	4
2.730	.0379	.0308	.417	3067	2499	1453	2699	2085	2098	5
2.107	.0085	-----	----	1874	1264	1123	1610	1296	----	6
3.396	.0331	.0267	.306	2182	1715	1267	1916	1443	1729	7
3.181	.0367	.0303	.377	2330	1853	1362	2033	1520	1944	8
2.973	.0427	.0363	.466	2514	2086	1512	2204	1635	2313	9
2.643	.0475	.0415	.637	2784	2343	1646	2427	1792	2792	10
1.918	.0087	-----	----	1430	833	1106	1188	901	----	11
3.114	.0350	.0289	.368	1706	1327	1294	1512	1088	1851	12
2.900	.0402	.0342	.452	1861	1501	1394	1641	1180	2166	13
2.673	.0445	.0386	.562	1998	1665	1512	1774	1271	2518	14
2.803	.0472	.0415	.509	2038	1686	1582	1798	1301	2513	15
2.419	.0514	.0462	.781	2215	1890	1687	1972	1407	3209	16
2.237	.0084	-----	----	1592	971	1119	1279	950	----	17
3.271	.0337	.0278	.322	1862	1441	1255	1630	1169	1741	18
3.194	.0351	.0291	.340	1894	1463	1272	1663	1195	1813	19
3.155	.0365	.0305	.354	1959	1527	1310	1709	1228	1872	20
2.834	.0421	.0360	.464	2180	1774	1450	1885	1373	2265	21
2.409	.0492	.0435	.716	2518	2105	1682	2203	1605	3019	22
1.997	.0081	-----	----	1798	1019	1112	1429	1027	----	23
3.147	.0319	.0258	.337	2022	1528	(a)	1781	1258	1719	24
3.071	.0341	.0279	.362	2064	1607	1290	1835	1300	1830	25
3.142	.0357	.0299	.350	2101	1634	1299	1850	1315	1849	26
2.678	.0414	.0352	.511	2410	1971	1464	2116	1522	2340	27
2.500	.0436	.0373	.613	2510	2090	1526	2225	1604	2602	28
2.462	.0463	.0404	.658	2567	2121	1625	2296	1690	2797	29
2.382	.0474	.0414	.697	2747	2292	1624	2412	1745	2913	30

Page intentionally left blank

Page intentionally left blank

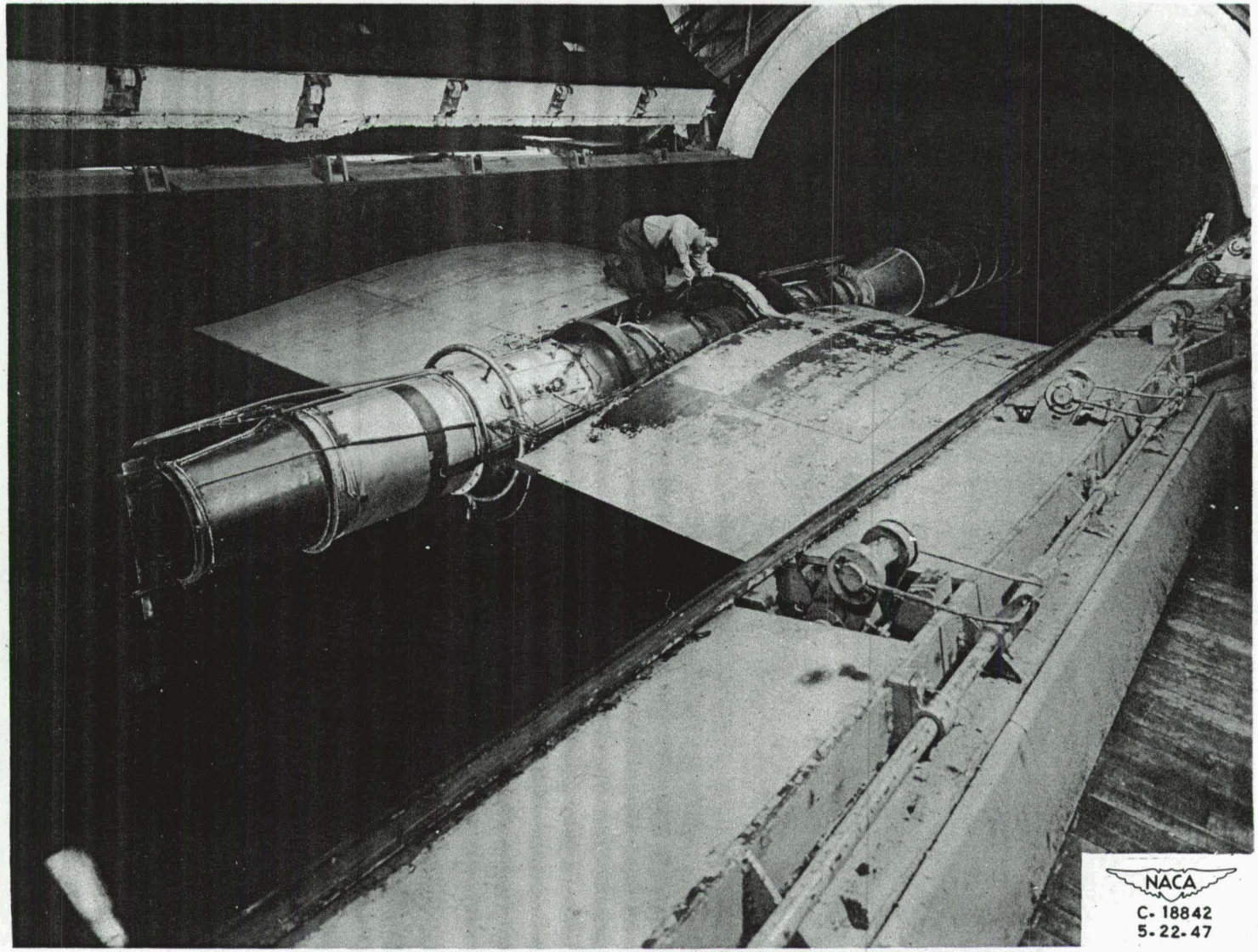

Figure 1. - Installation of turbojet engine with $25\frac{3}{4}$-inch-diameter tail-pipe burner in altitude wind tunnel.

Page intentionally left blank

Page intentionally left blank

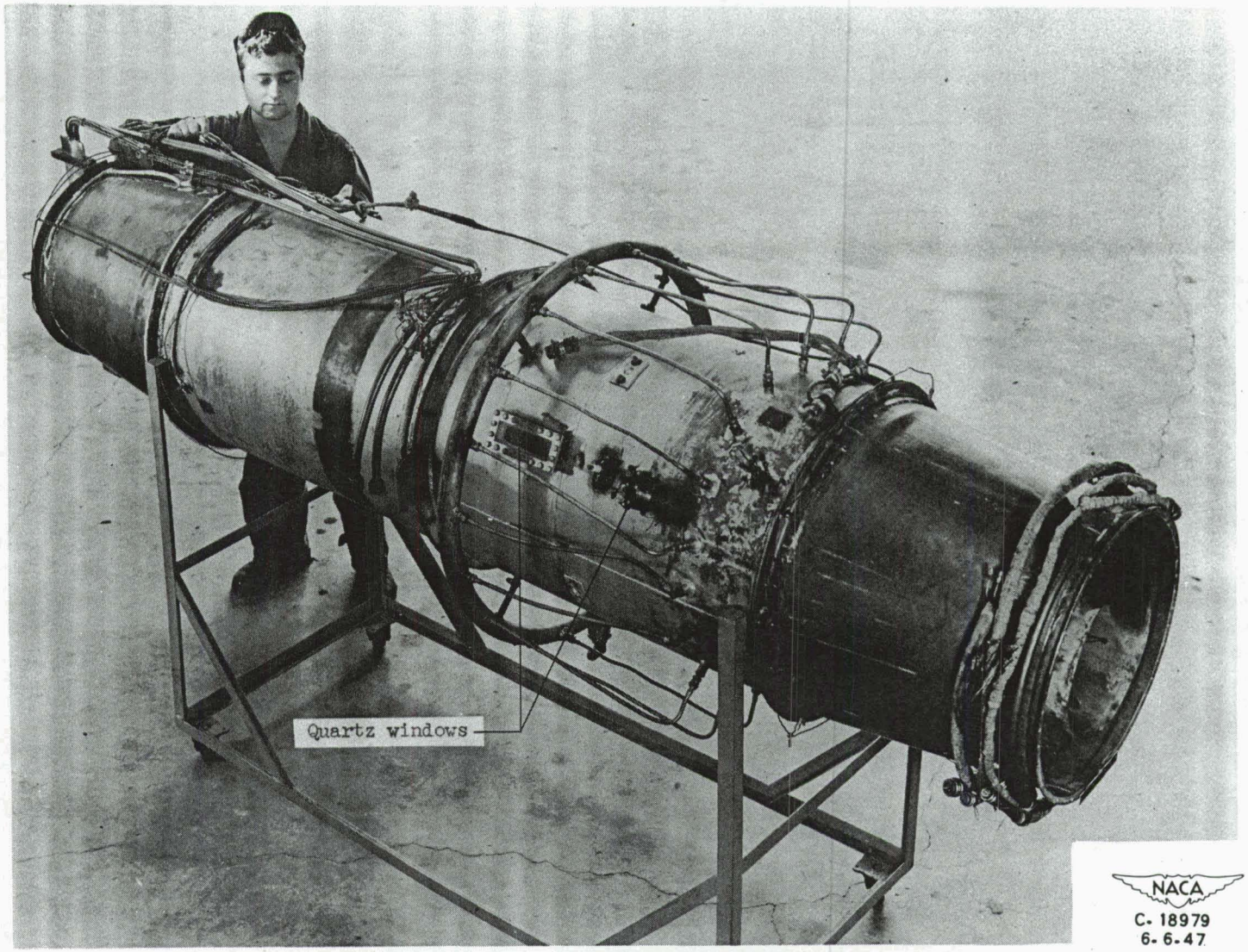

Figure 2. - Tail pipe used with configurations A, B, and C.

Page intentionally left blank

Page intentionally left blank

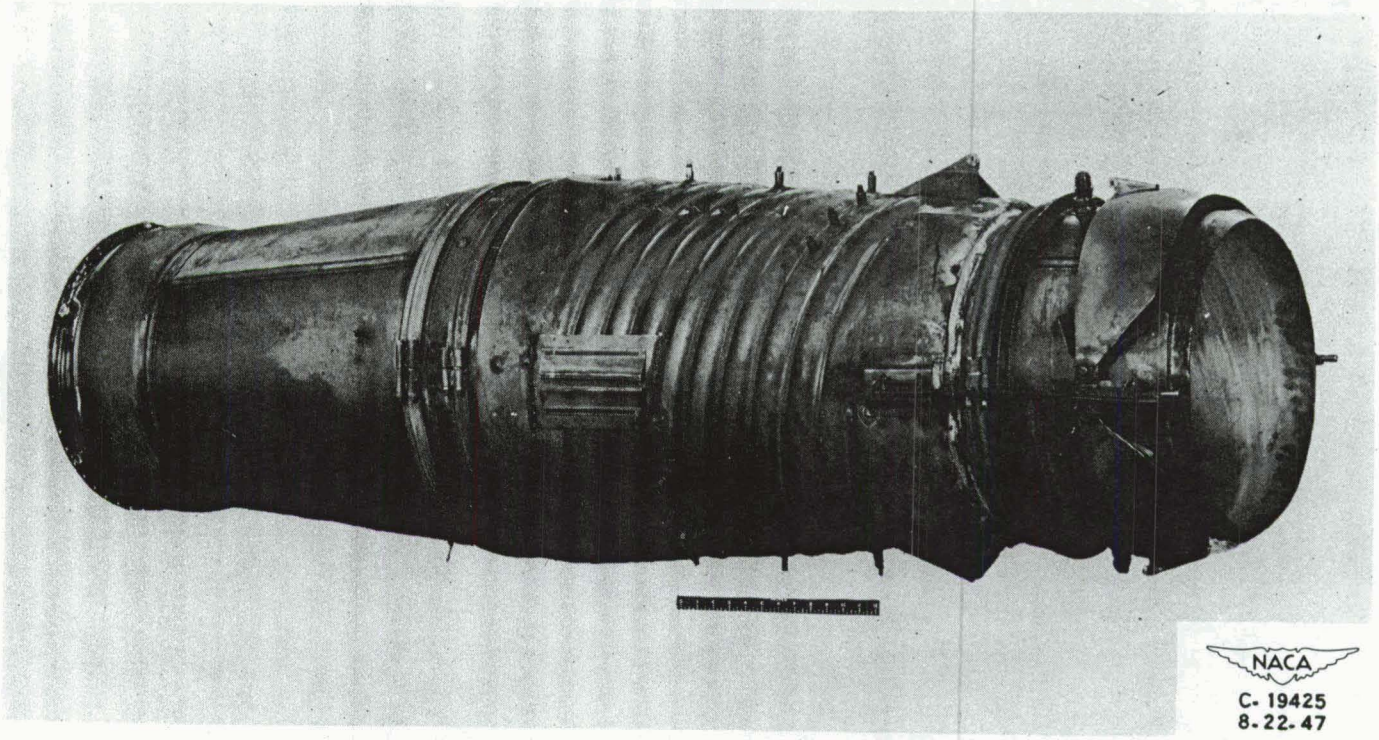

Figure 3. - Tail pipe used with configuration D.

Page intentionally left blank

Page intentionally left blank

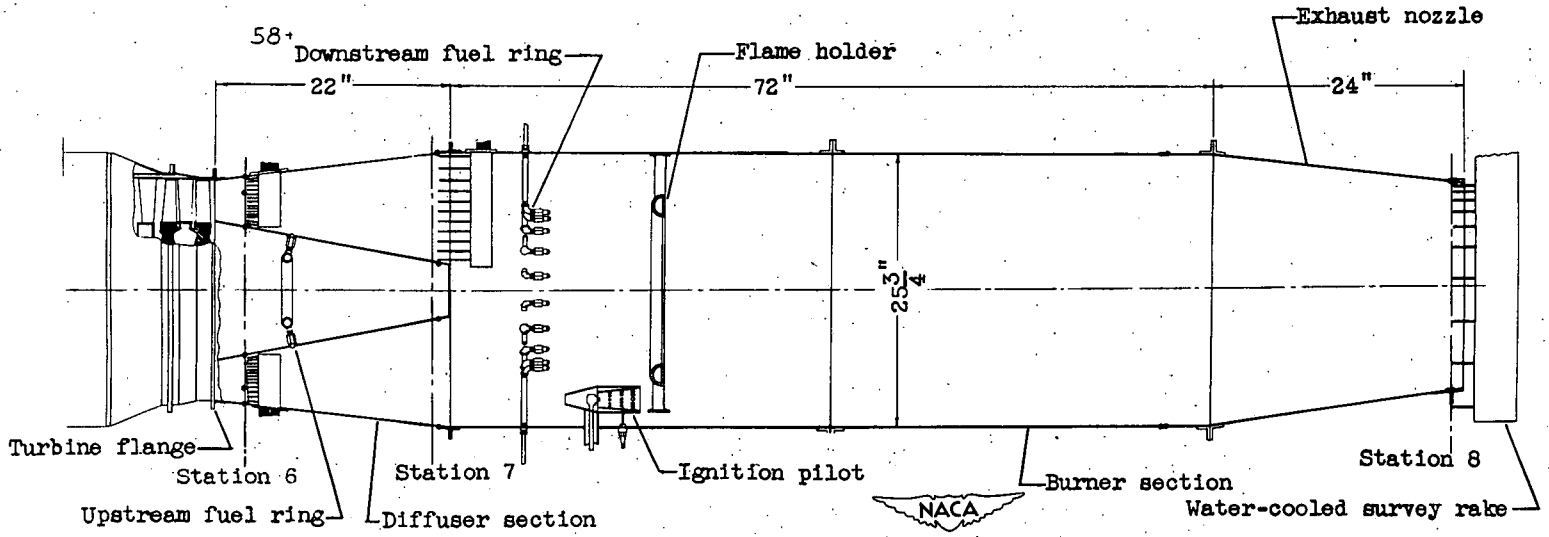

Figure 4. - Cross section of configuration A with $25\frac{3}{4}$-inch-diameter tail pipe.

Page intentionally left blank

Page intentionally left blank

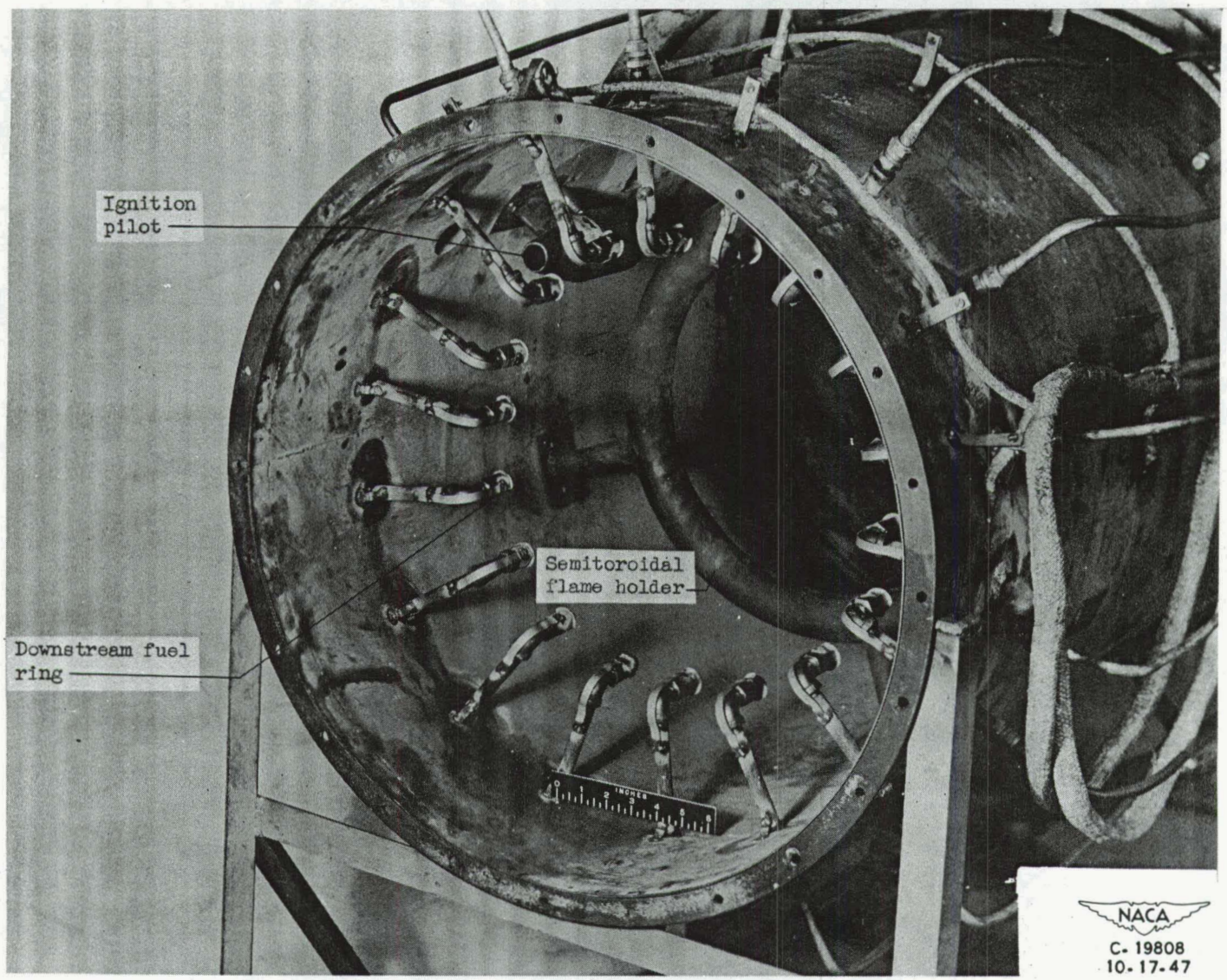

Figure 5. - Downstream fuel ring and semitoroidal flame holder, configuration A (looking downstream).

Page intentionally left blank

Page intentionally left blank

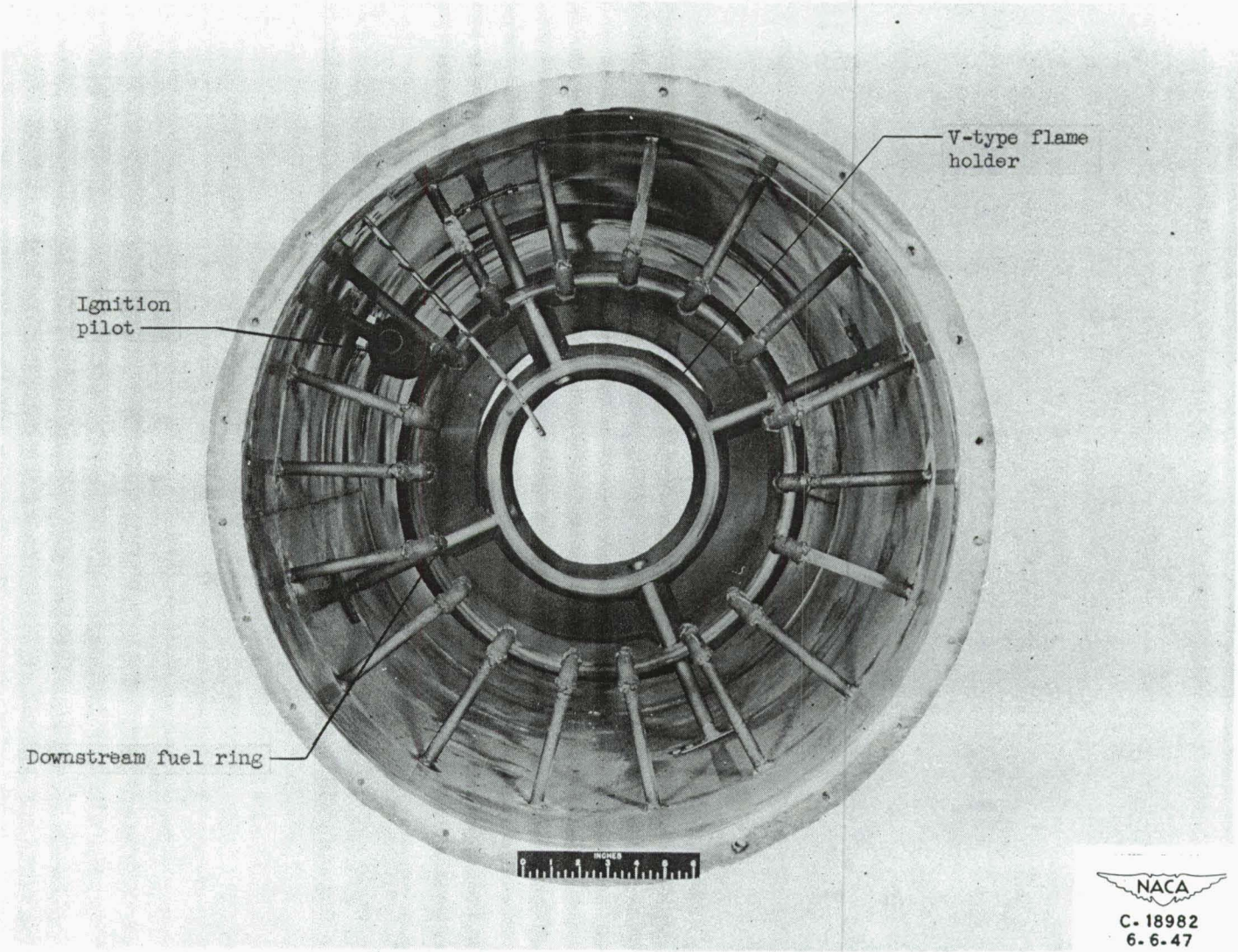

Figure 6. - Downstream fuel ring and annular V-type flame holder, configuration B (looking downstream).

Page intentionally left blank

Page intentionally left blank

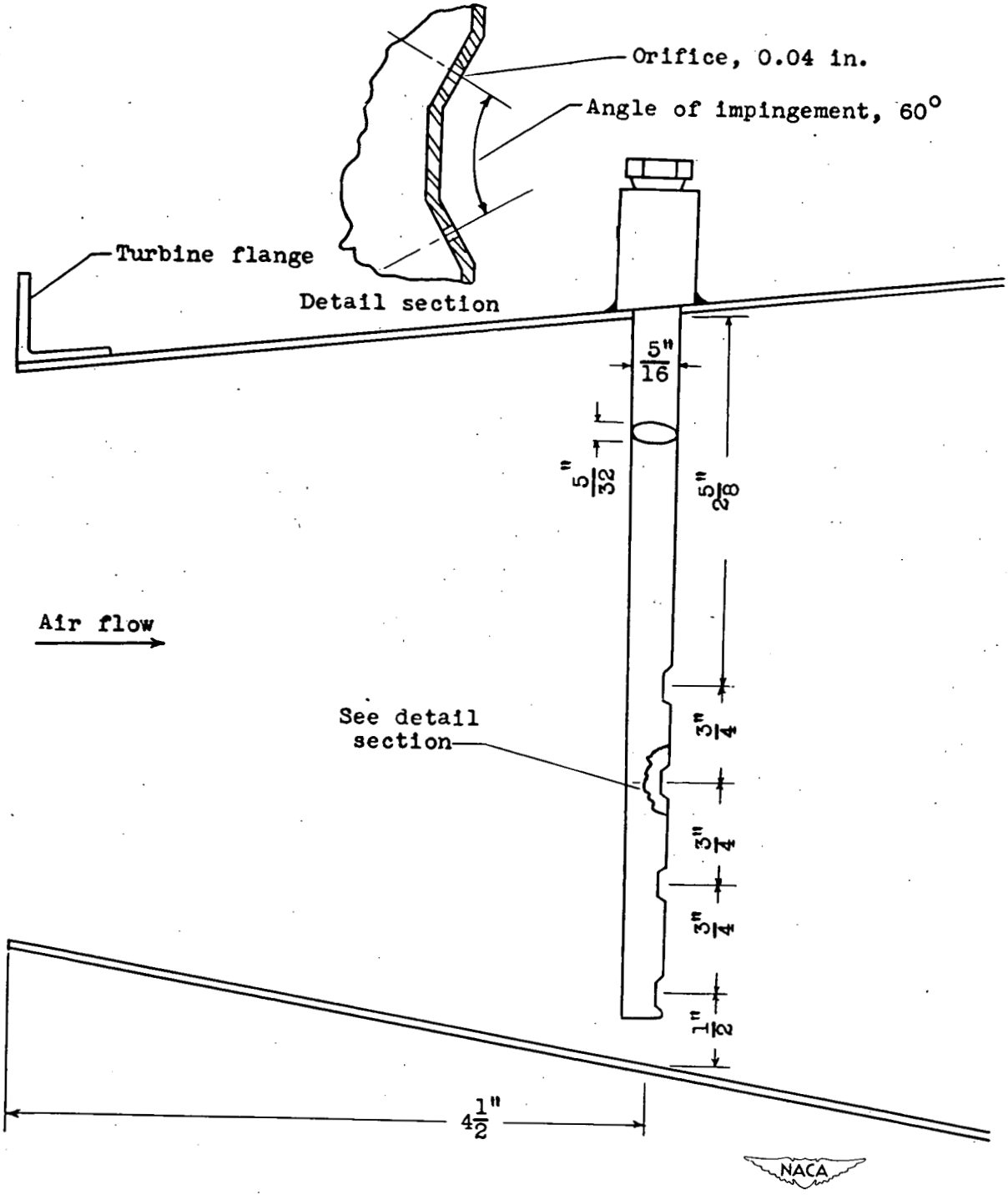

Figure 7. - Details of impinging jet spray bars installed in diffuser section for configuration C.

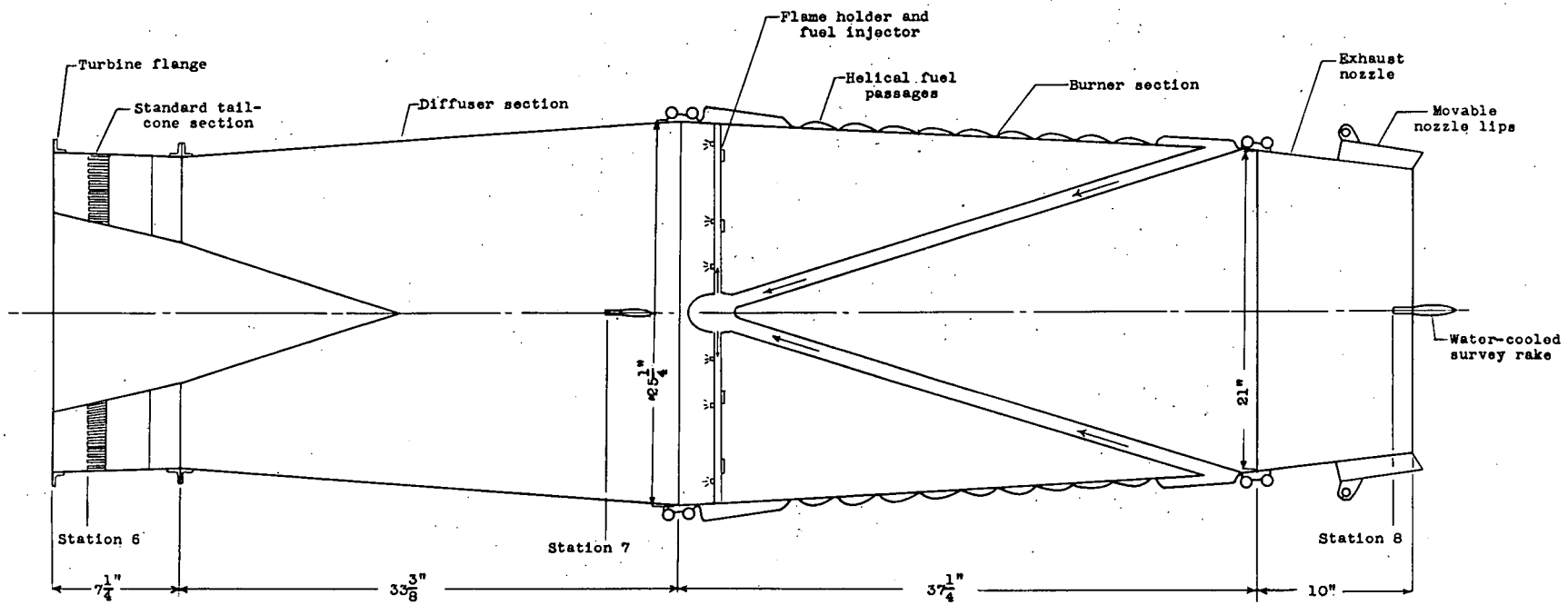

Figure 8. - Cross section of tail-pipe burner of configuration D.

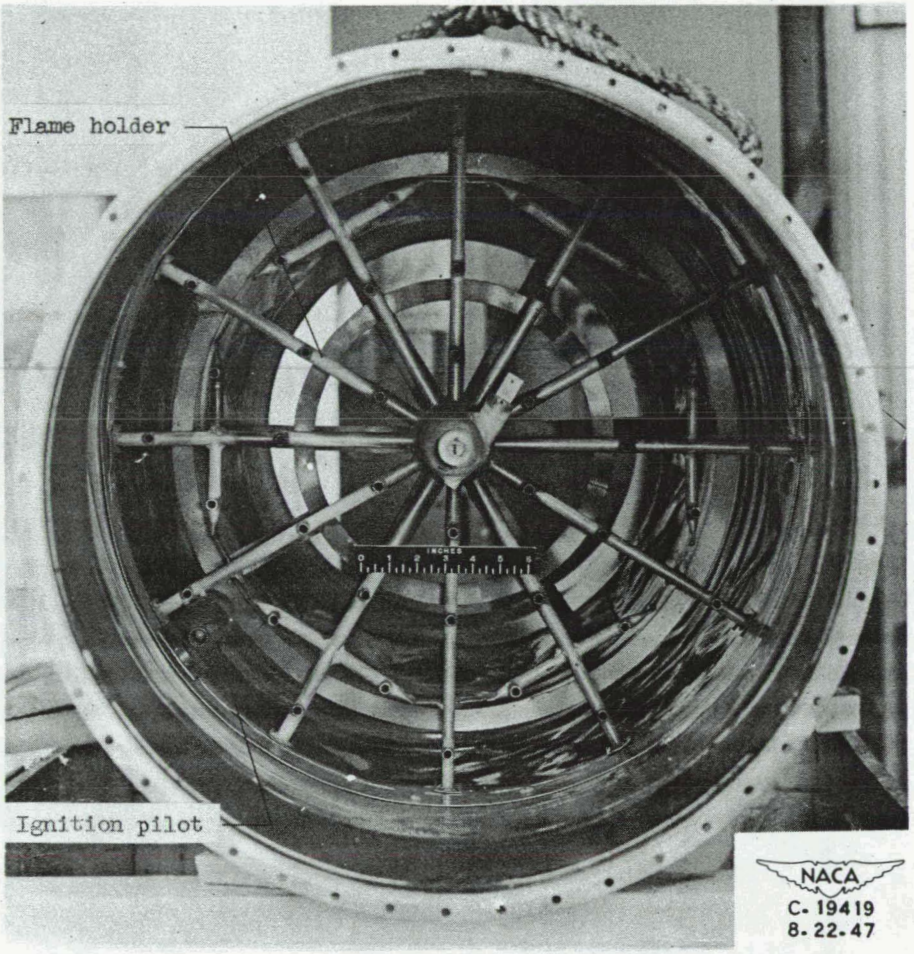

Figure 9. - Fuel-injection system and flame holder, configuration D (looking downstream).

Page intentionally left blank

Page intentionally left blank

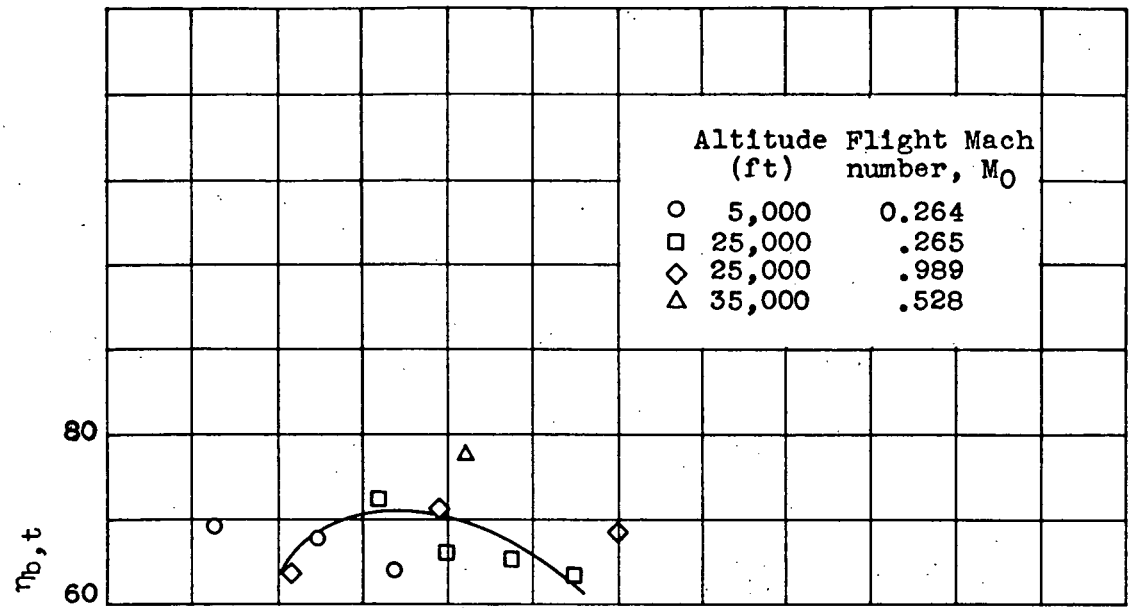

(a) Configuration A.

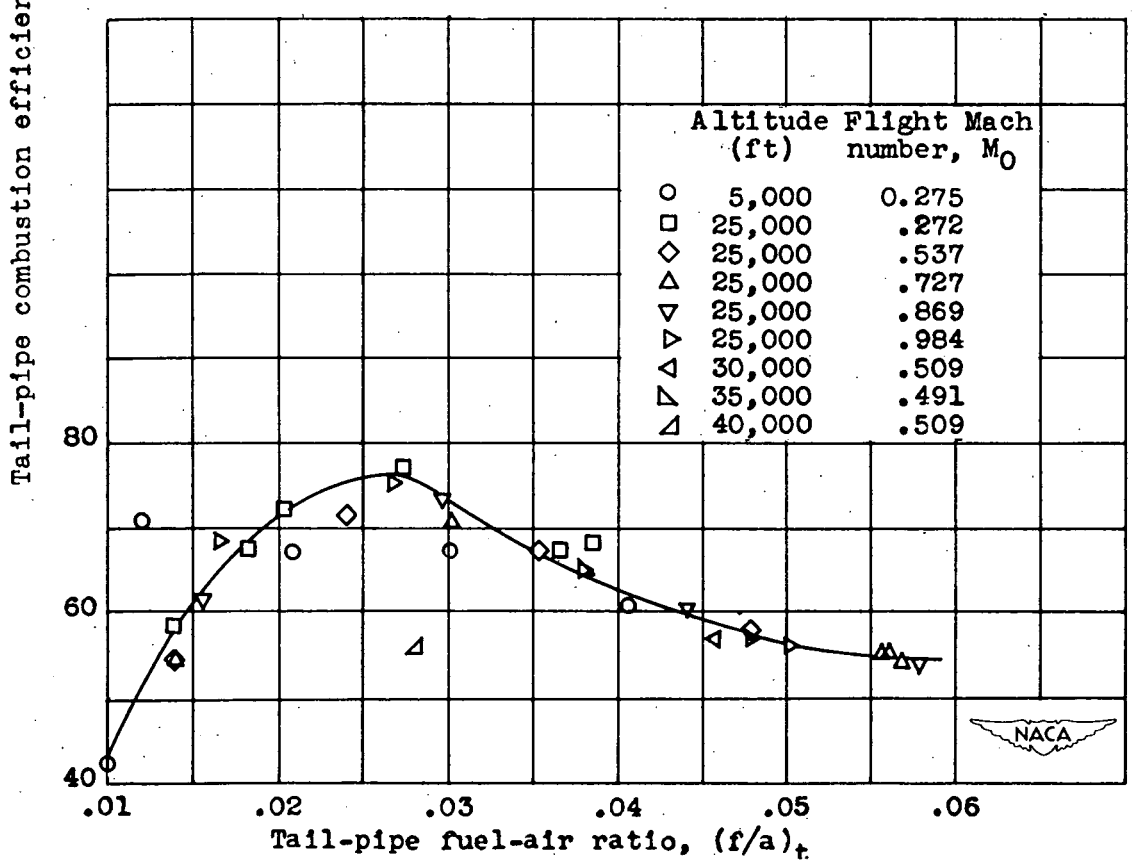

(b) Configuration B.

Figure 10. - Variation of tail-pipe combustion efficiency with tail-pipe fuel-air ratio for four configurations.

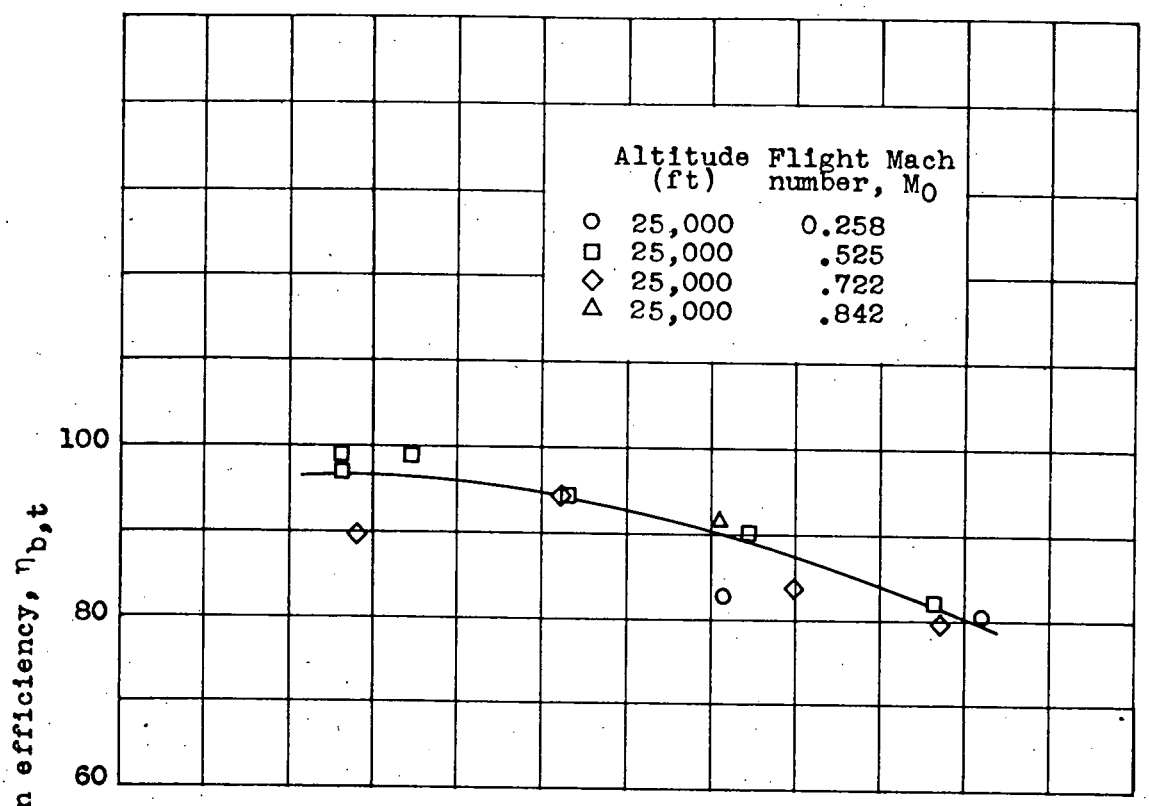

(c) Configuration C.

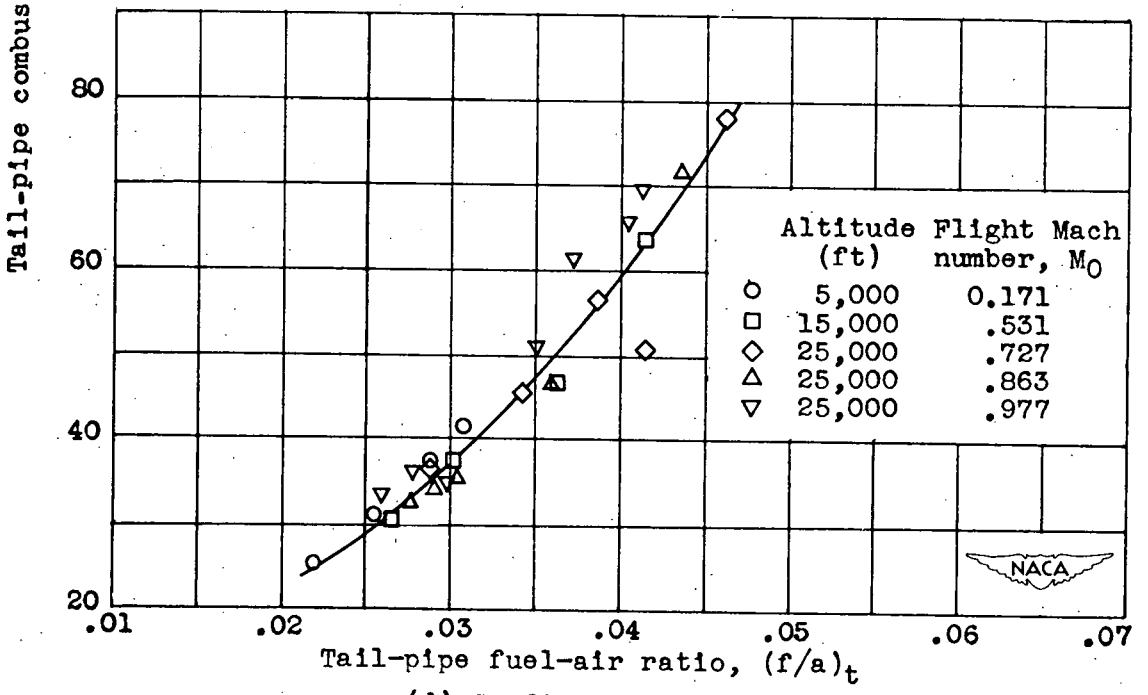

(d) Configuration D.

Figure 10. - Concluded. Variation of tail-pipe combustion efficiency with tail-pipe fuel-air ratio for four configurations.

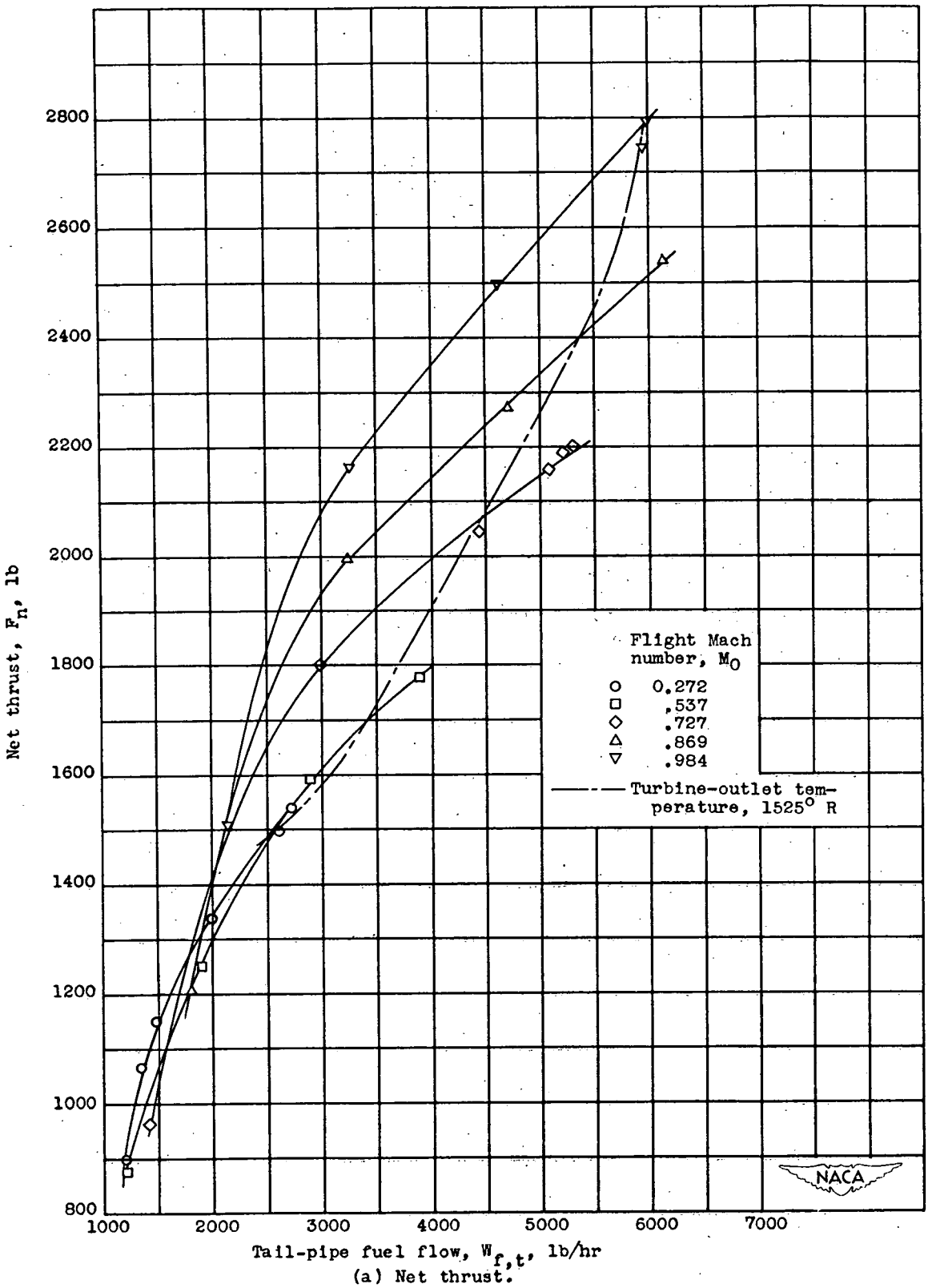

(a) Net thrust.

Figure 11. - Variation of performance parameters with tail-pipe fuel flow for several flight Mach numbers. Configuration B; altitude, 25,000 feet; engine speed, 12,500 rpm.

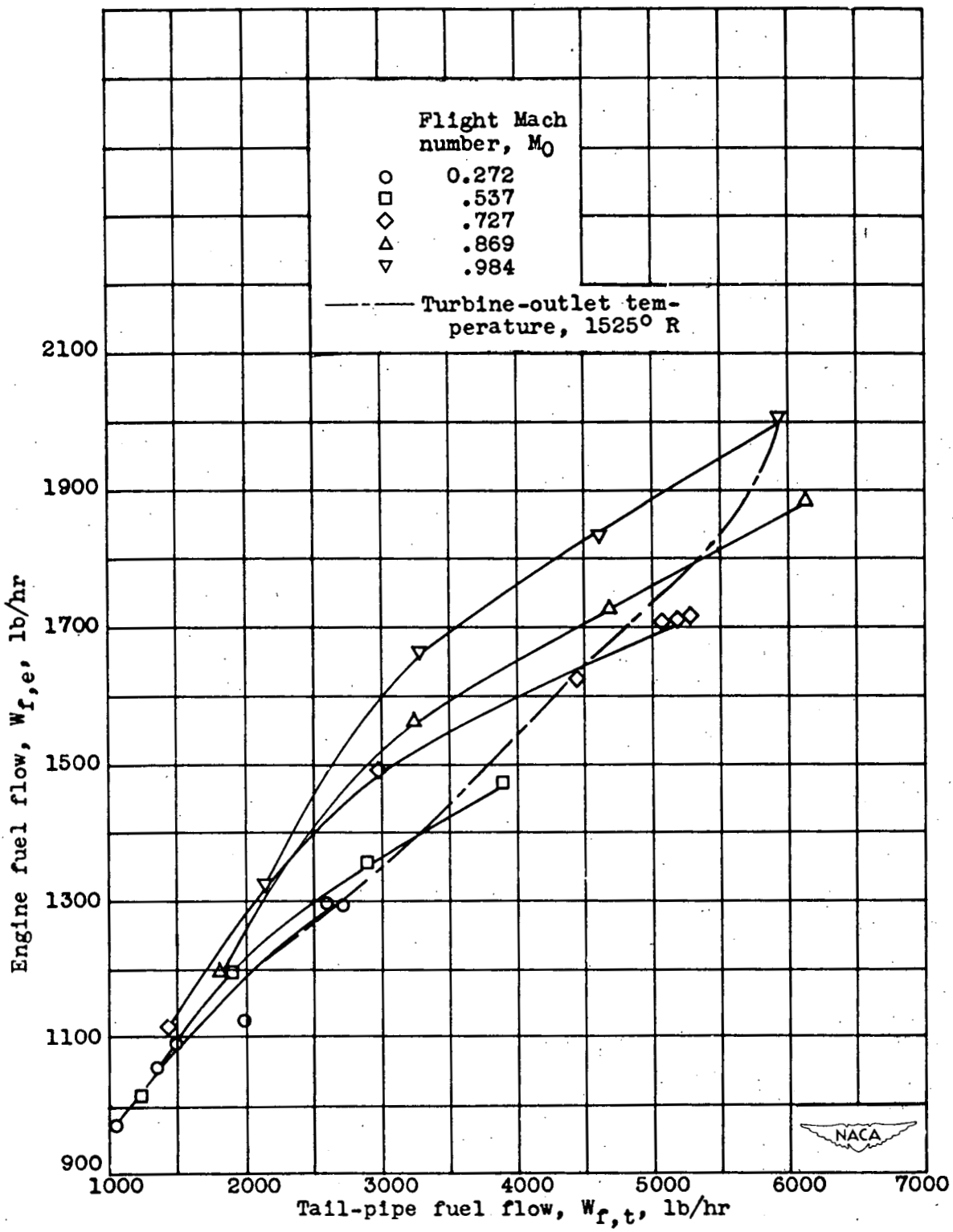

(b) Engine fuel flow.

Figure 11. - Continued. Variation of performance parameters with tail-pipe fuel flow for several flight Mach numbers. Configuration B; altitude, 25,000 feet; engine speed, 12,500 rpm.

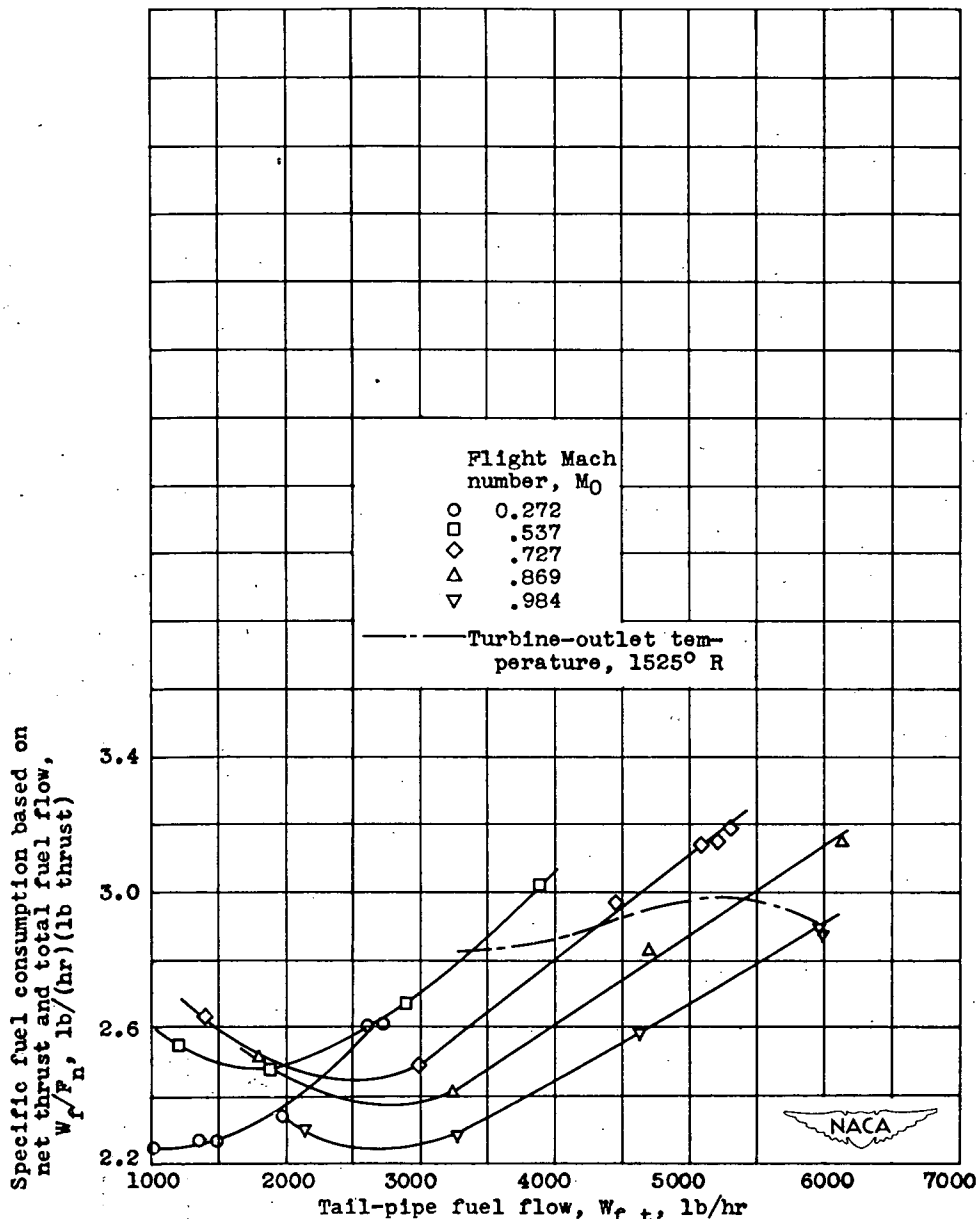

(c) Specific fuel consumption based on net thrust and total fuel flow.

Figure 11. - Continued. Variation of performance parameters with tail-pipe fuel flow for several flight Mach numbers. Configuration B; altitude, 25,000 feet; engine speed, 12,500 rpm.

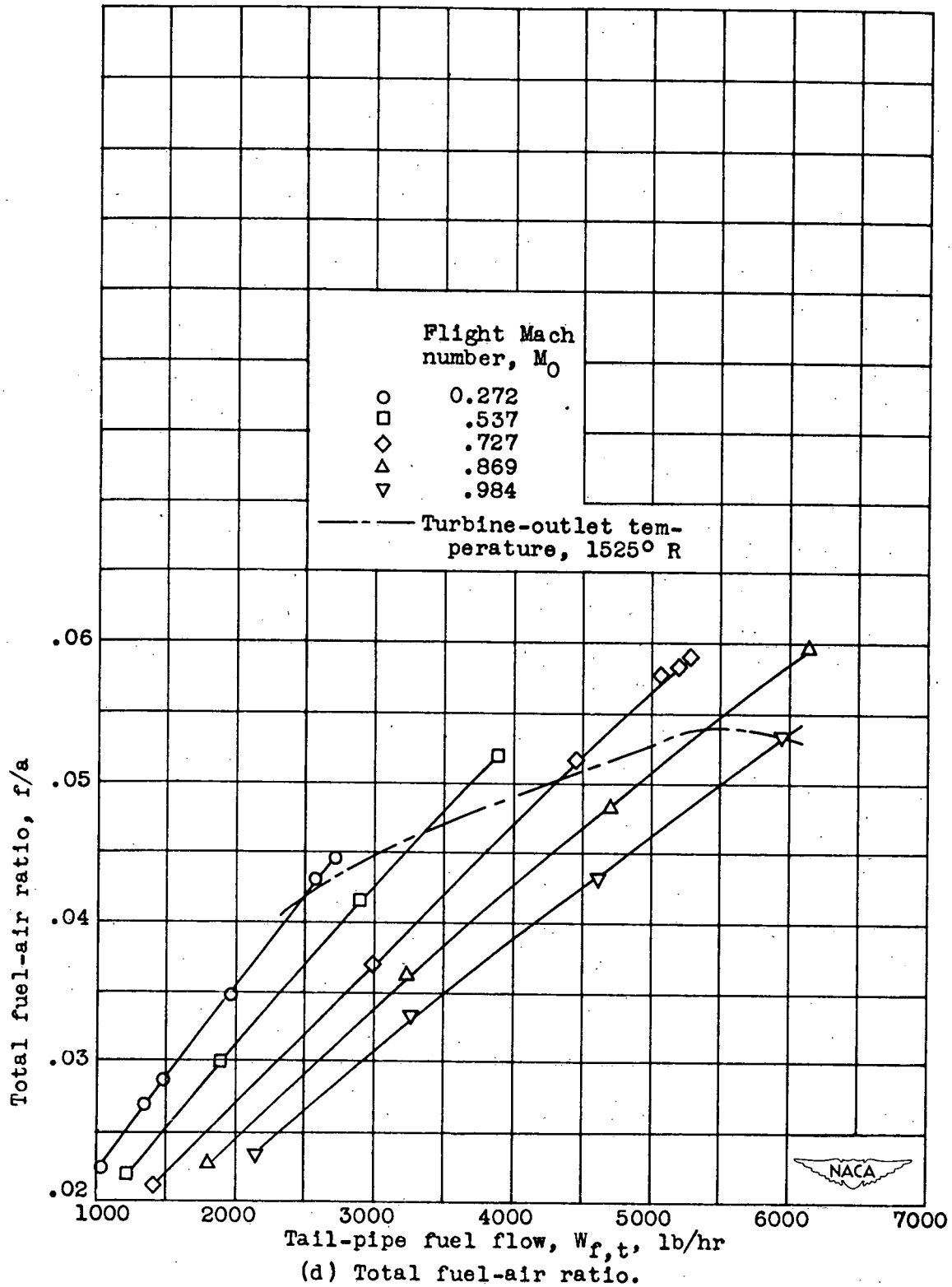

(d) Total fuel-air ratio.

Figure 11. - Continued. Variation of performance parameters with tail-pipe fuel flow for several flight Mach numbers. Configuration B; altitude, 25,000 feet; engine speed, 12,500 rpm.

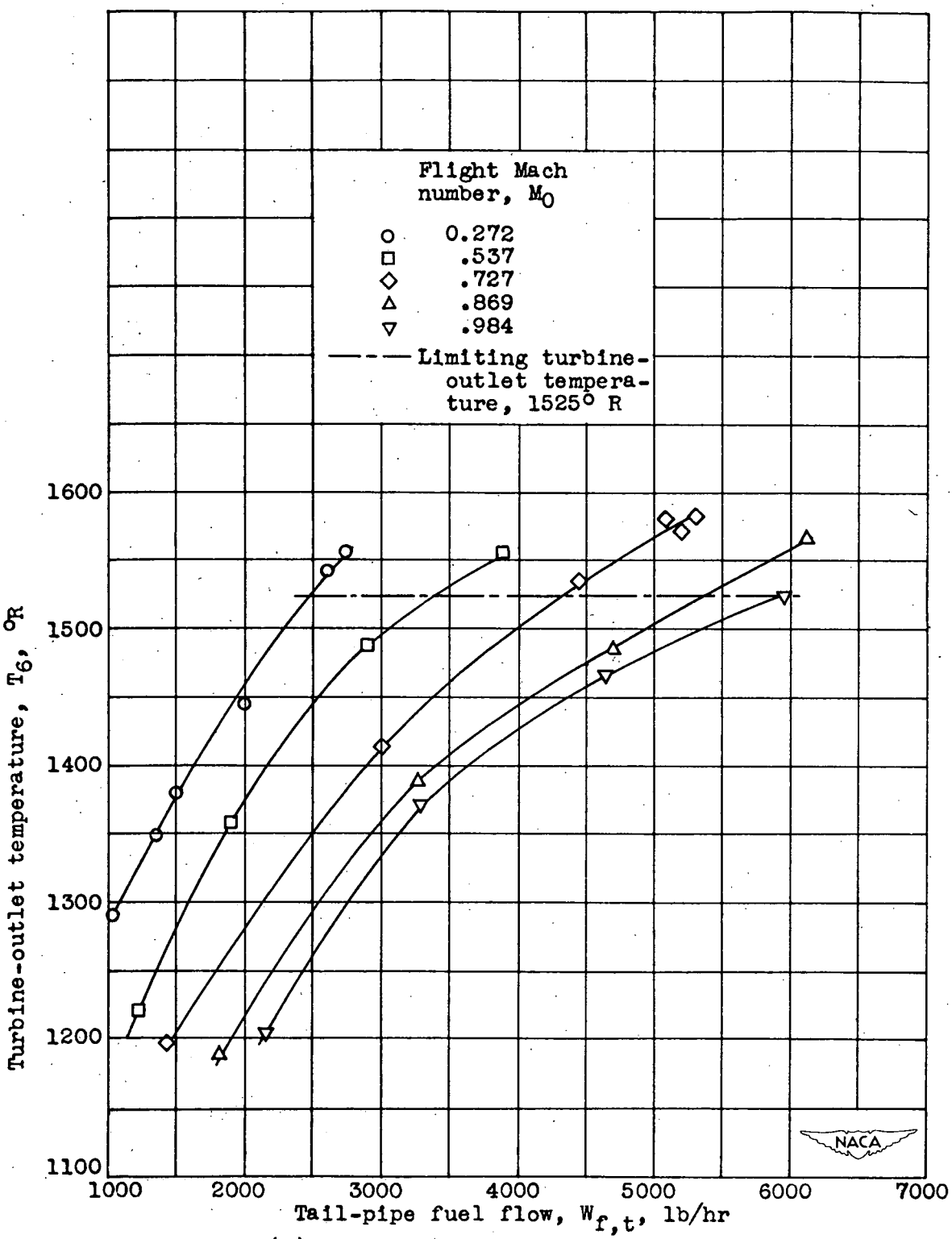

(e) Turbine-outlet temperature.

Figure 11. - Continued. Variation of performance parameters with tail-pipe fuel flow for several flight Mach numbers. Configuration B; altitude, 25,000 feet; engine speed, 12,500 rpm.

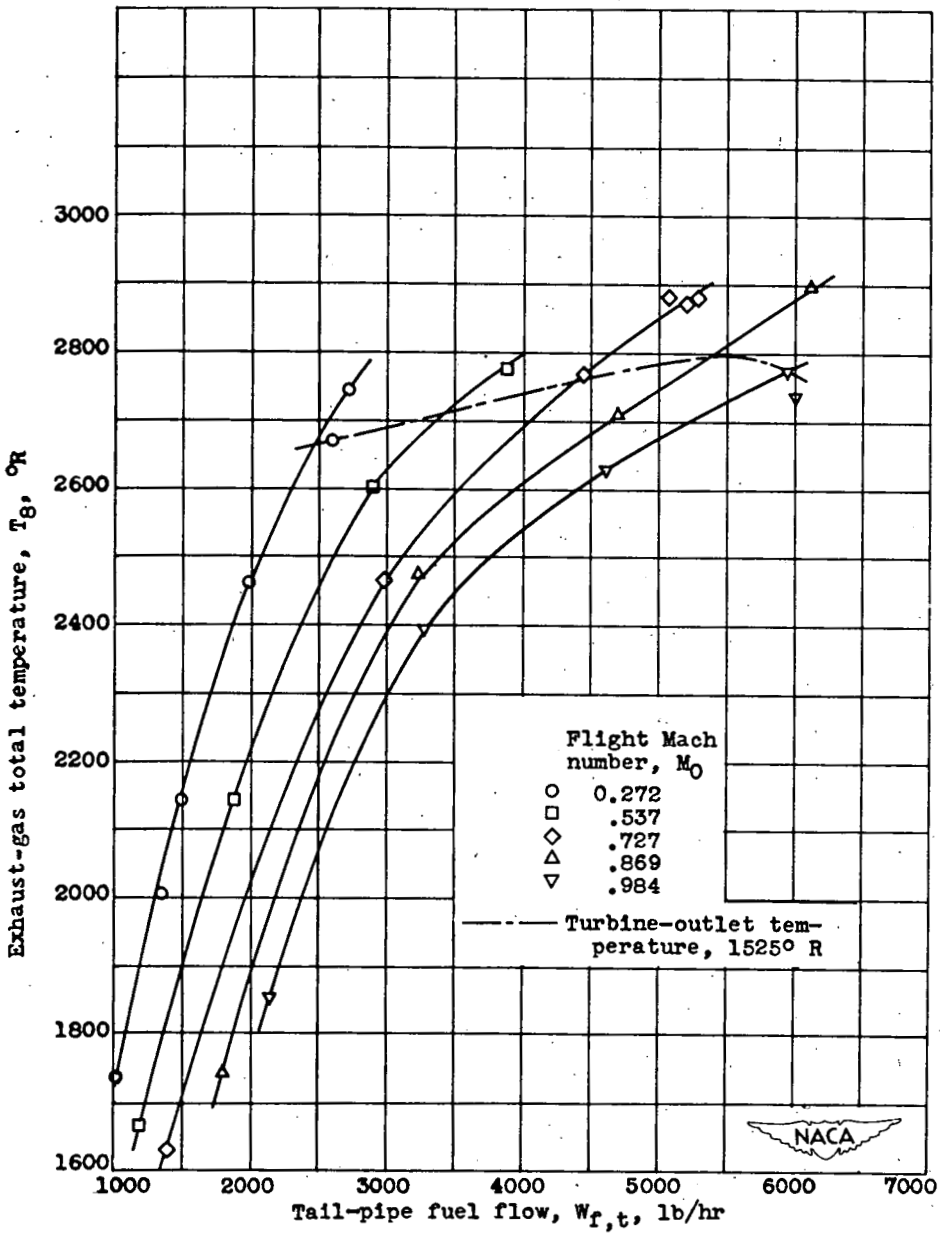

(f) Exhaust-gas total temperature.

Figure 11. - Concluded. Variation of performance parameters with tail-pipe fuel flow for several flight Mach numbers. Configuration B; altitude, 25,000 feet; engine speed, 12,500 rpm.

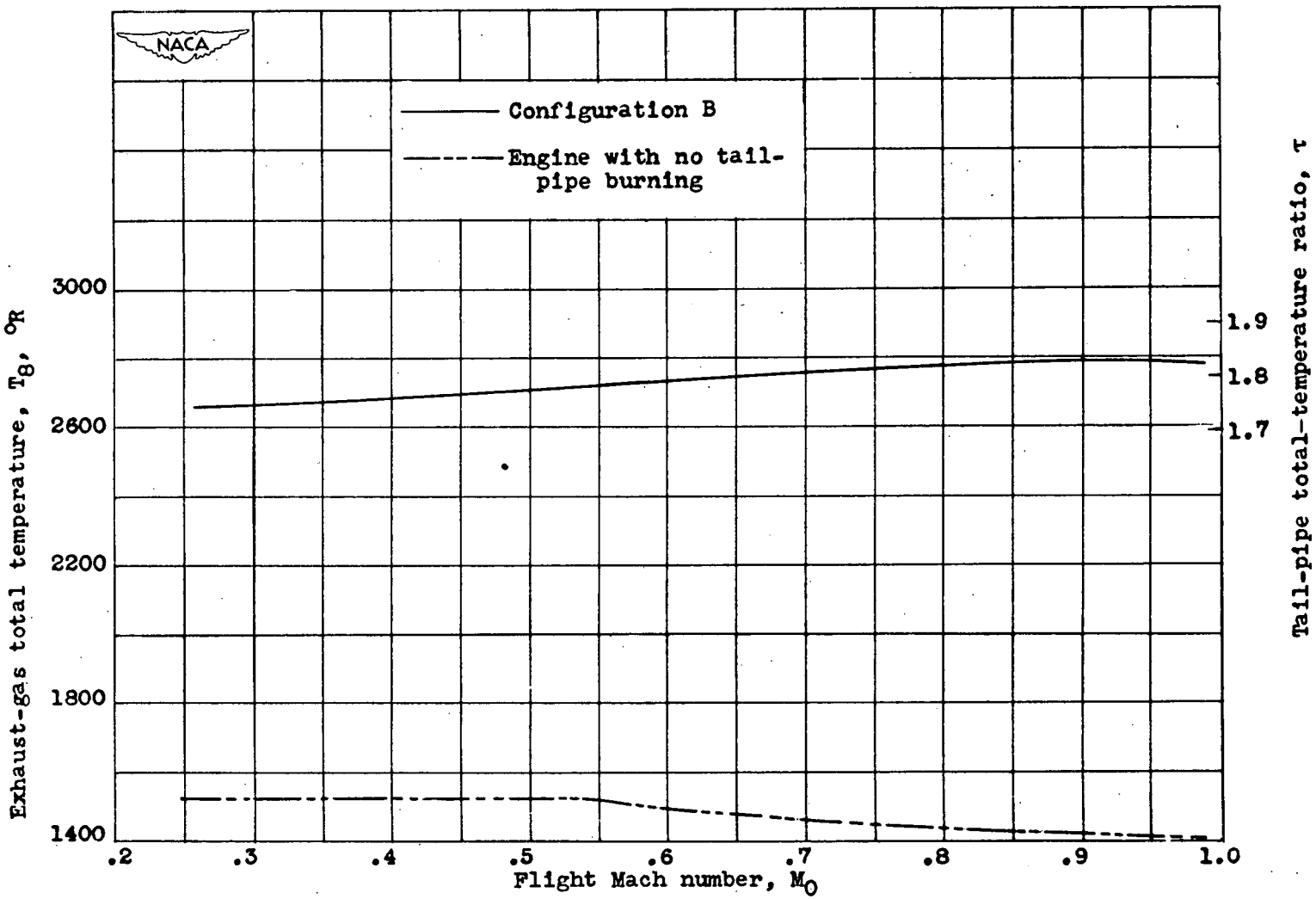

(a) Configuration B; original engine; turbine-outlet temperature, T_6, 1525° R.

Figure 12. - Relation between exhaust-gas total temperature and flight Mach number with standard tail pipe and with modified tail pipe and tail-pipe burning. Altitude, 25,000 feet; engine speed, 12,500 rpm.

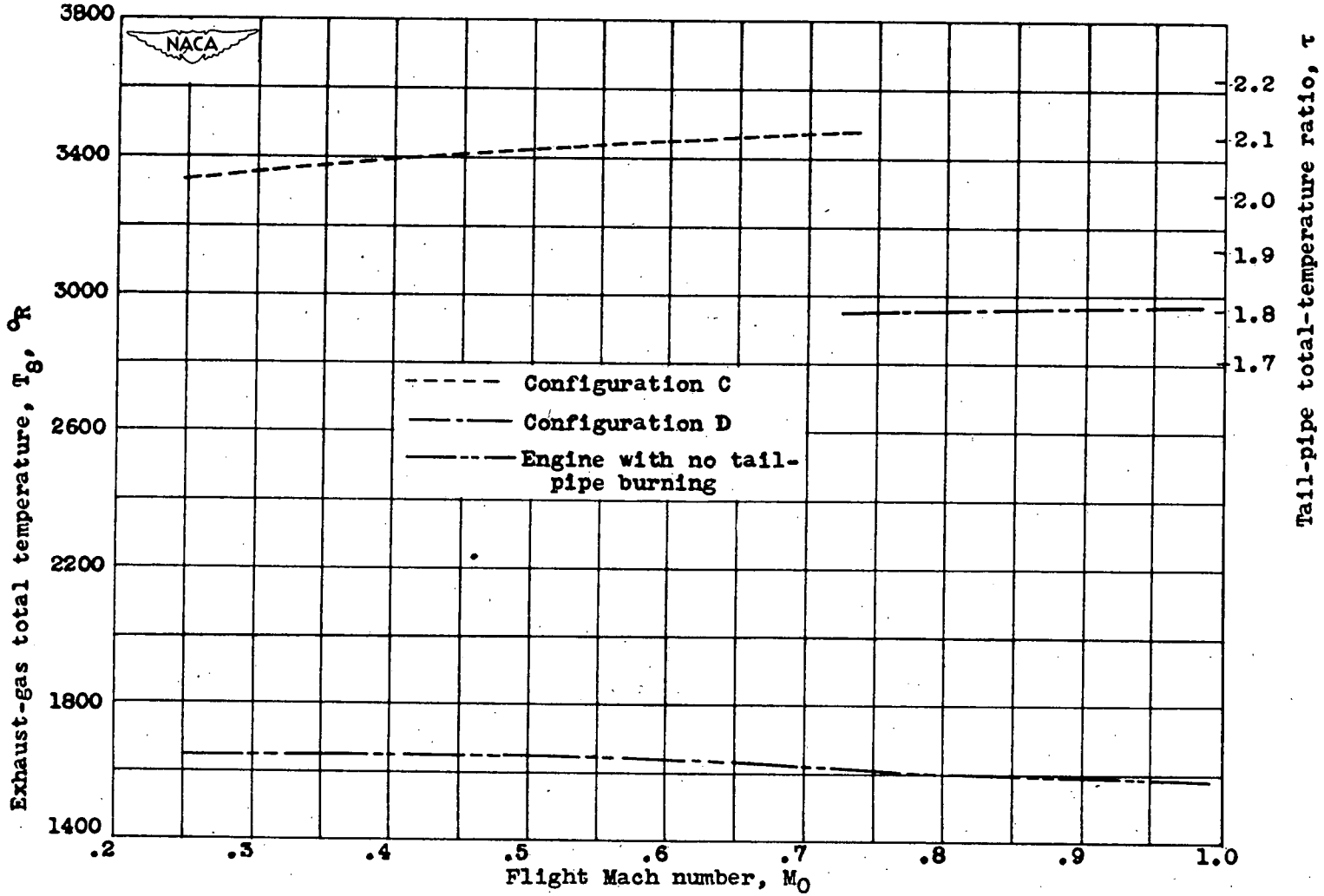

(b) Configurations C and D; modified engine; turbine-outlet temperature, T_6, 1650° R.

Figure 12. - Concluded. Relation between exhaust-gas total temperature and flight Mach number with standard tail pipe and with modified tail pipe and tail-pipe burning. Altitude, 25,000 feet; engine speed, 12,500 rpm.

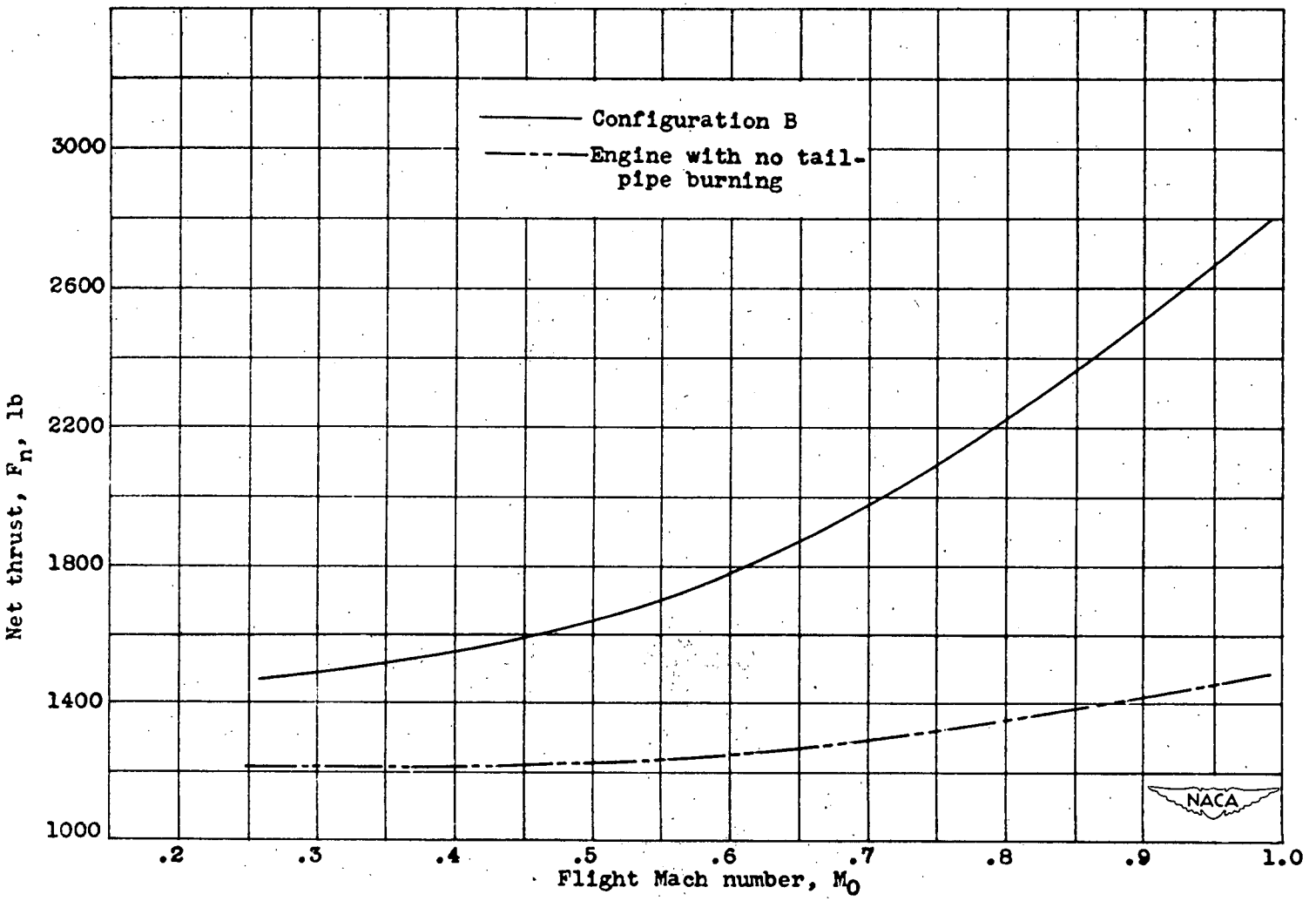

(a) Configuration B; original engine; turbine-outlet temperature with tail-pipe burning, T_6, 1525° R.

Figure 13. - Relation between net thrust and flight Mach number with standard tail pipe and with modified tail pipe and tail-pipe burning. Altitude, 25,000 feet; engine speed, 12,500 rpm.

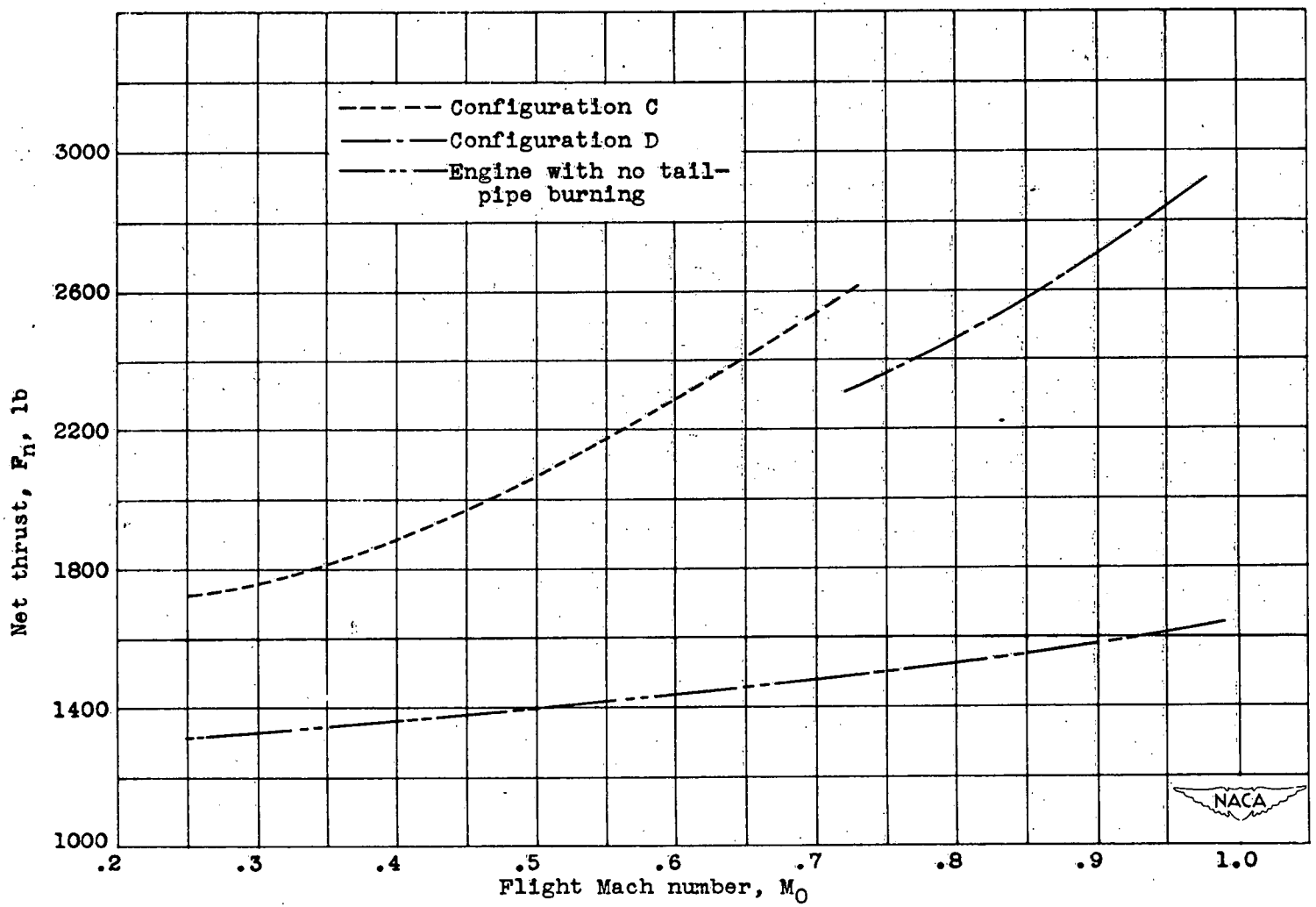

(b) Configurations C and D; modified engine; turbine-outlet temperature with tail-pipe burning, T_6, 1650° R.

Figure 13. - Concluded. Relation between net thrust and flight Mach number with standard tail pipe and with modified tail pipe and tail-pipe burning. Altitude, 25,000 feet; engine speed, 12,500 rpm.

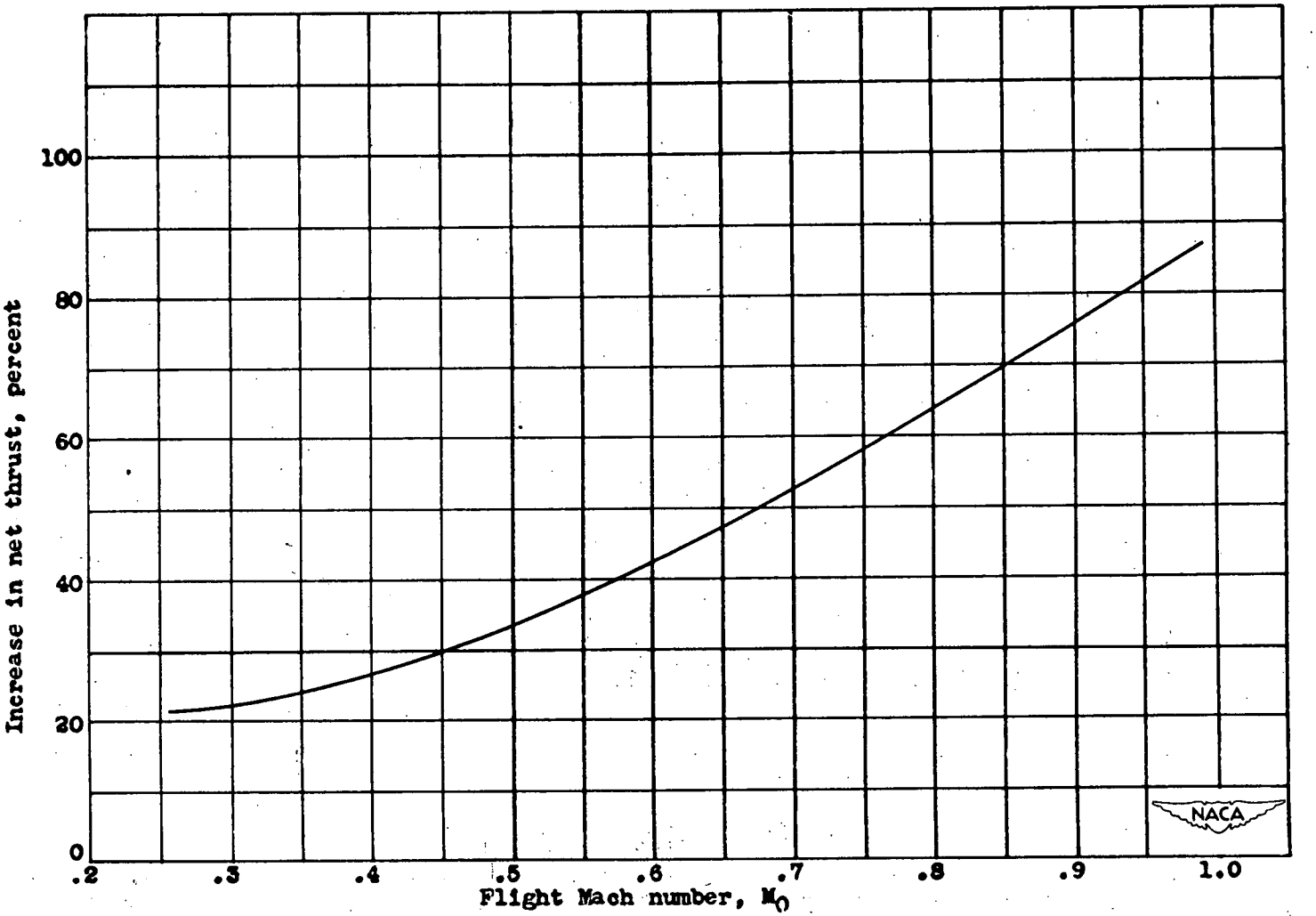

(a) Configuration B; original engine; turbine-outlet temperature with tail-pipe burning, T_6, 1525° R.

Figure 14. - Relation between increase in net thrust and flight Mach number with tail-pipe burning. Altitude, 25,000 feet; engine speed, 12,500 rpm.

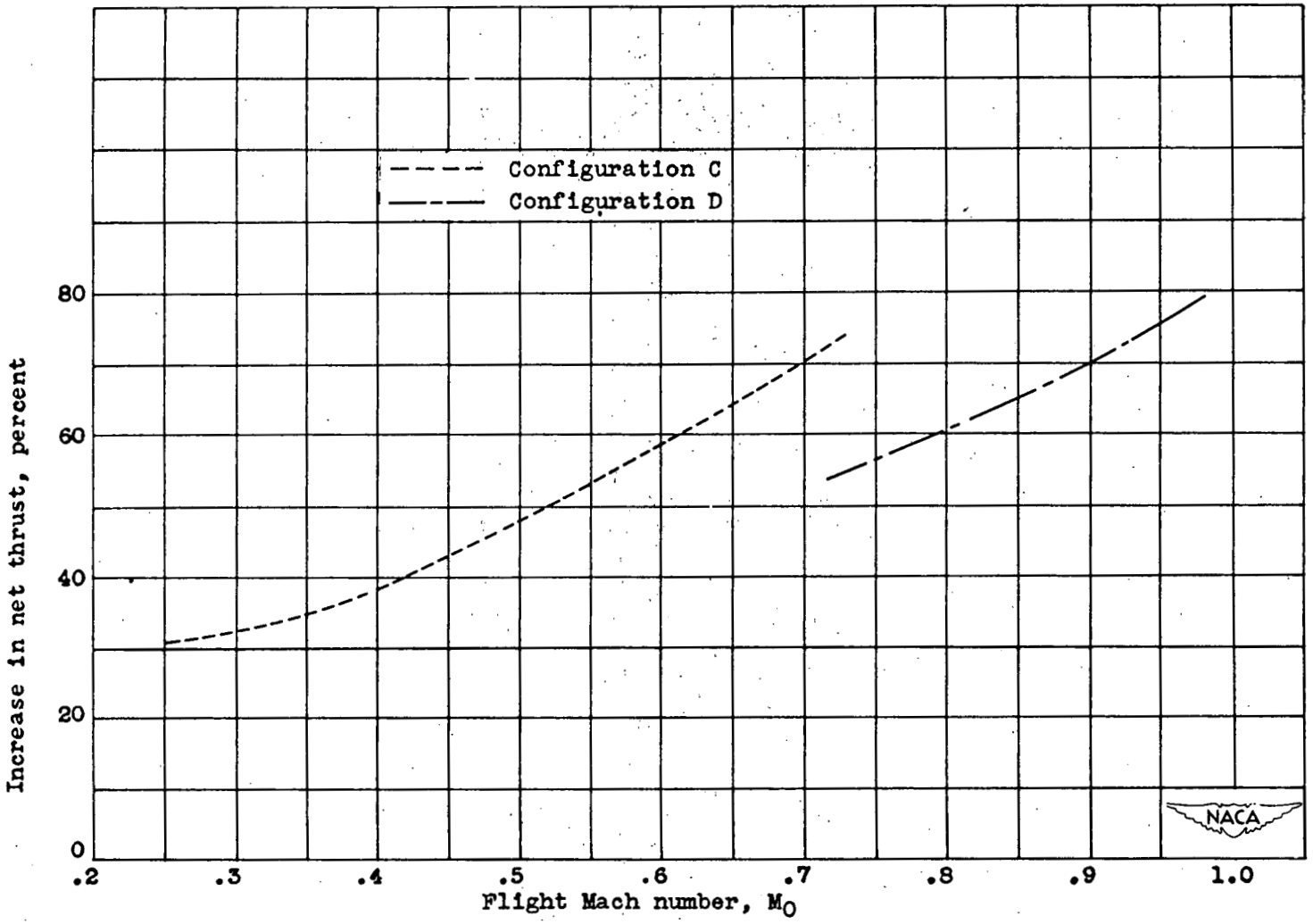

(b) Configurations C and D; modified engine; turbine-outlet temperature with tail-pipe burning, T_6, 1650° R.

Figure 14. - Concluded. Relation between increase in net thrust and flight Mach number with tail-pipe burning. Altitude, 25,000 feet; engine speed, 12,500 rpm.

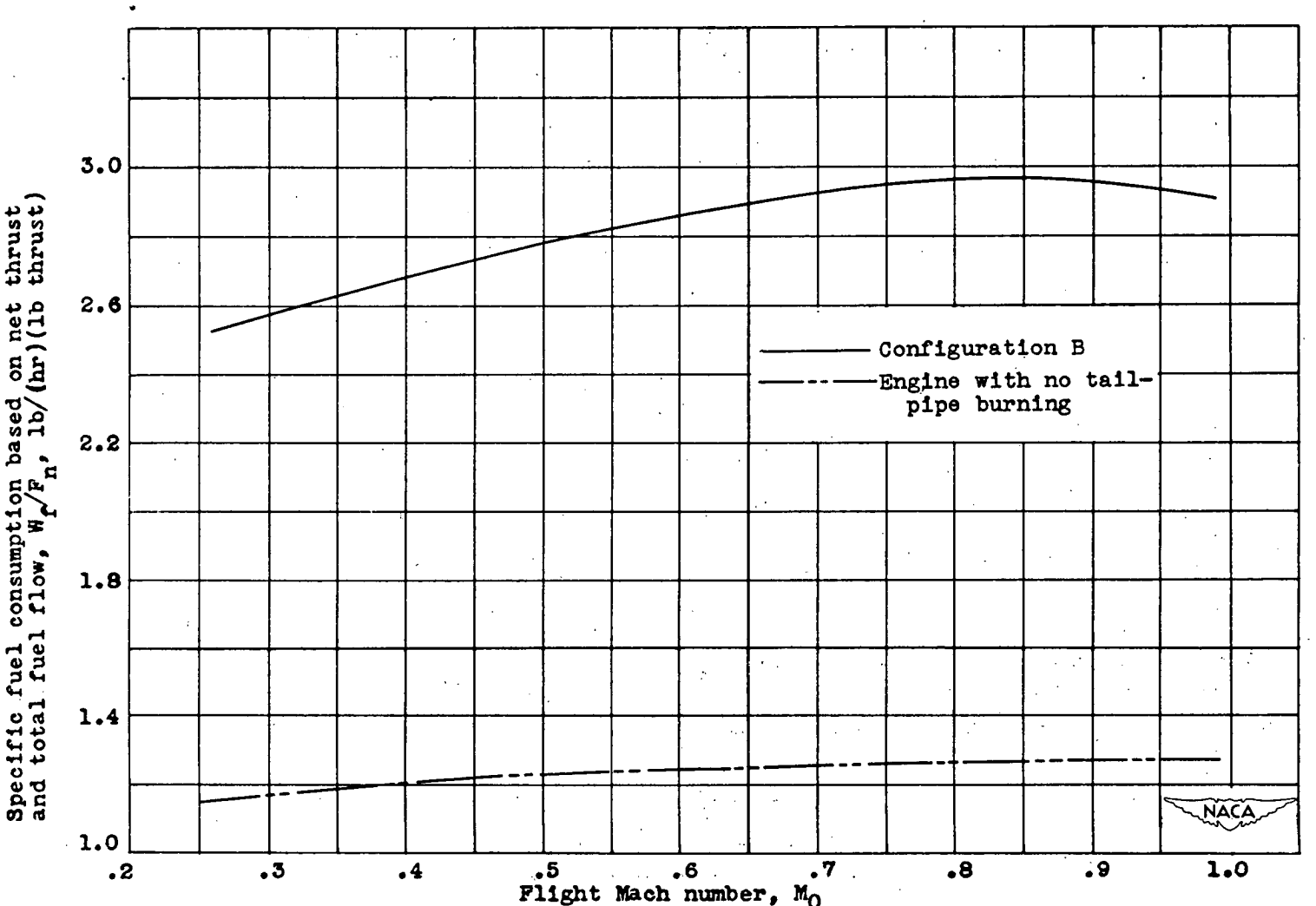

(a) Configuration B; original engine; turbine-outlet temperature, T_6, 1525° R.

Figure 15. - Relation between specific fuel consumption based on net thrust and total fuel flow and flight Mach number with standard tail pipe and with modified tail pipe and tail-pipe burning. Altitude, 25,000 feet; engine speed, 12,500 rpm.

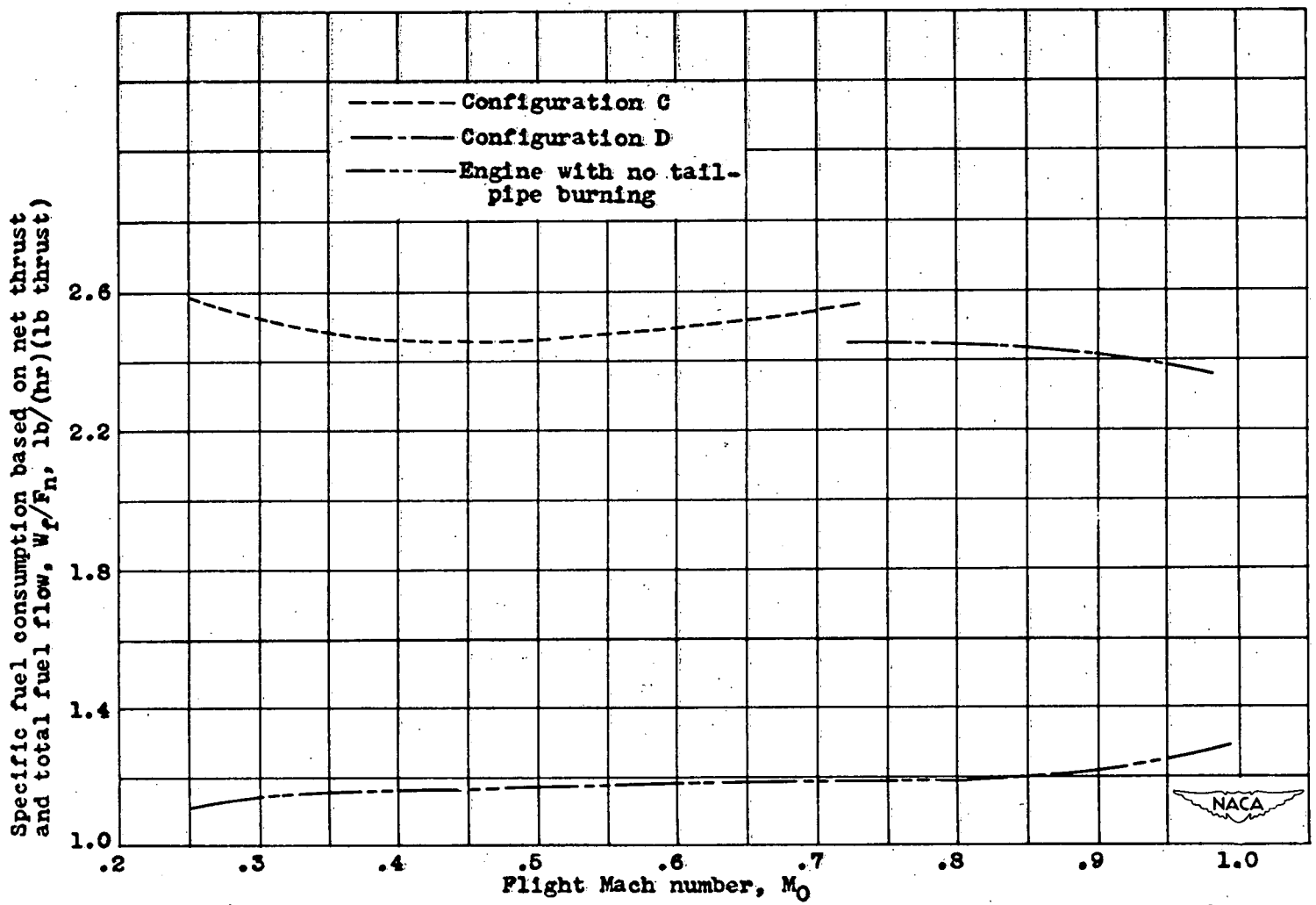

(b) Configurations C and D; modified engine; turbine-outlet temperature, T_6, 1650° R.

Figure 15. - Concluded. Relation between specific fuel consumption based on net thrust and total fuel flow and flight Mach number with standard tail pipe and with modified tail pipe and tail-pipe burning. Altitude, 25,000 feet; engine speed, 12,500 rpm.

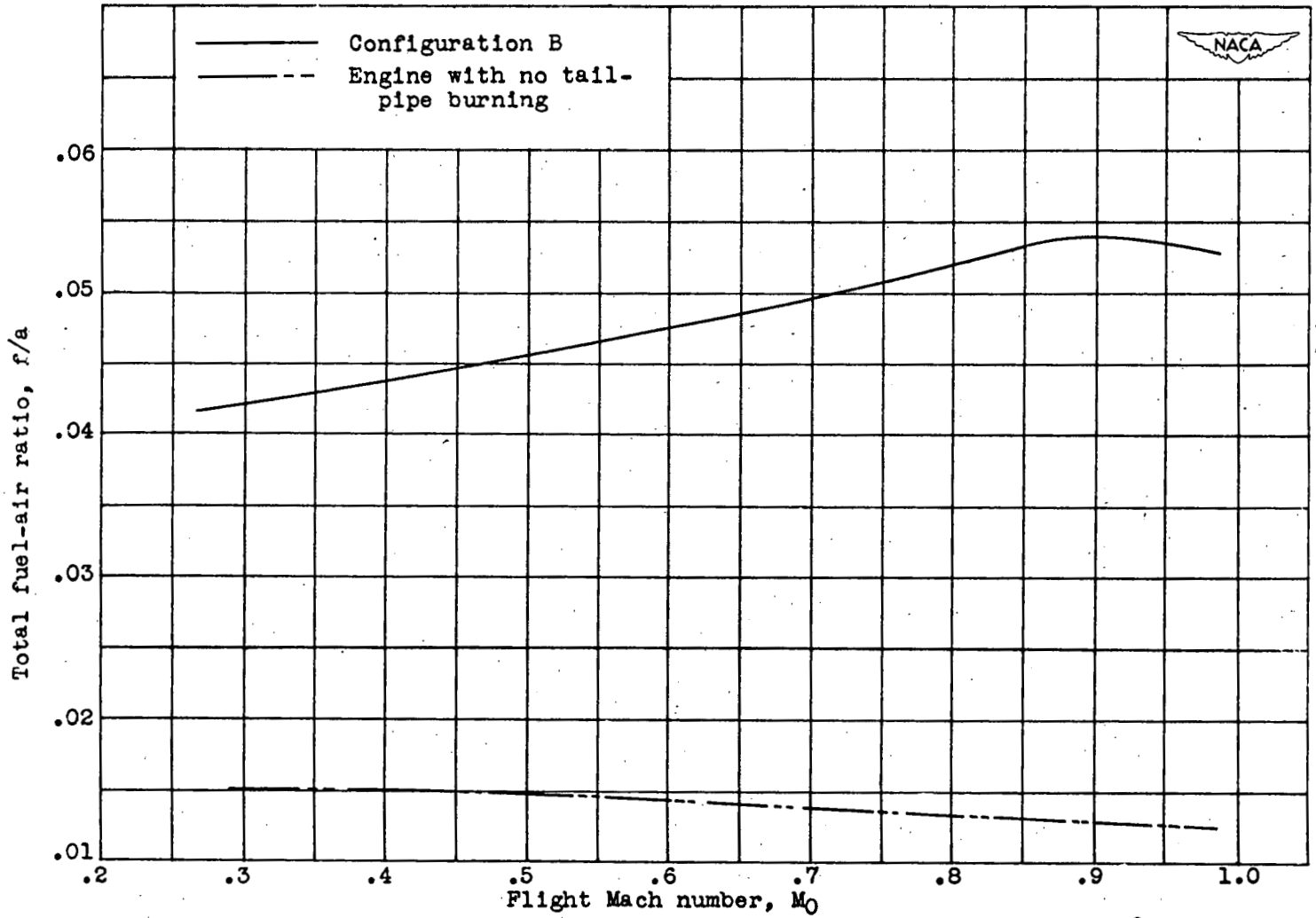

(a) Configuration B; original engine; turbine-outlet temperature, T_6, 1525° R.

Figure 16. - Relation between total fuel-air ratio and flight Mach number with standard tail pipe and with modified tail pipe and tail-pipe burning. Altitude, 25,000 feet; engine speed, 12,500 rpm.

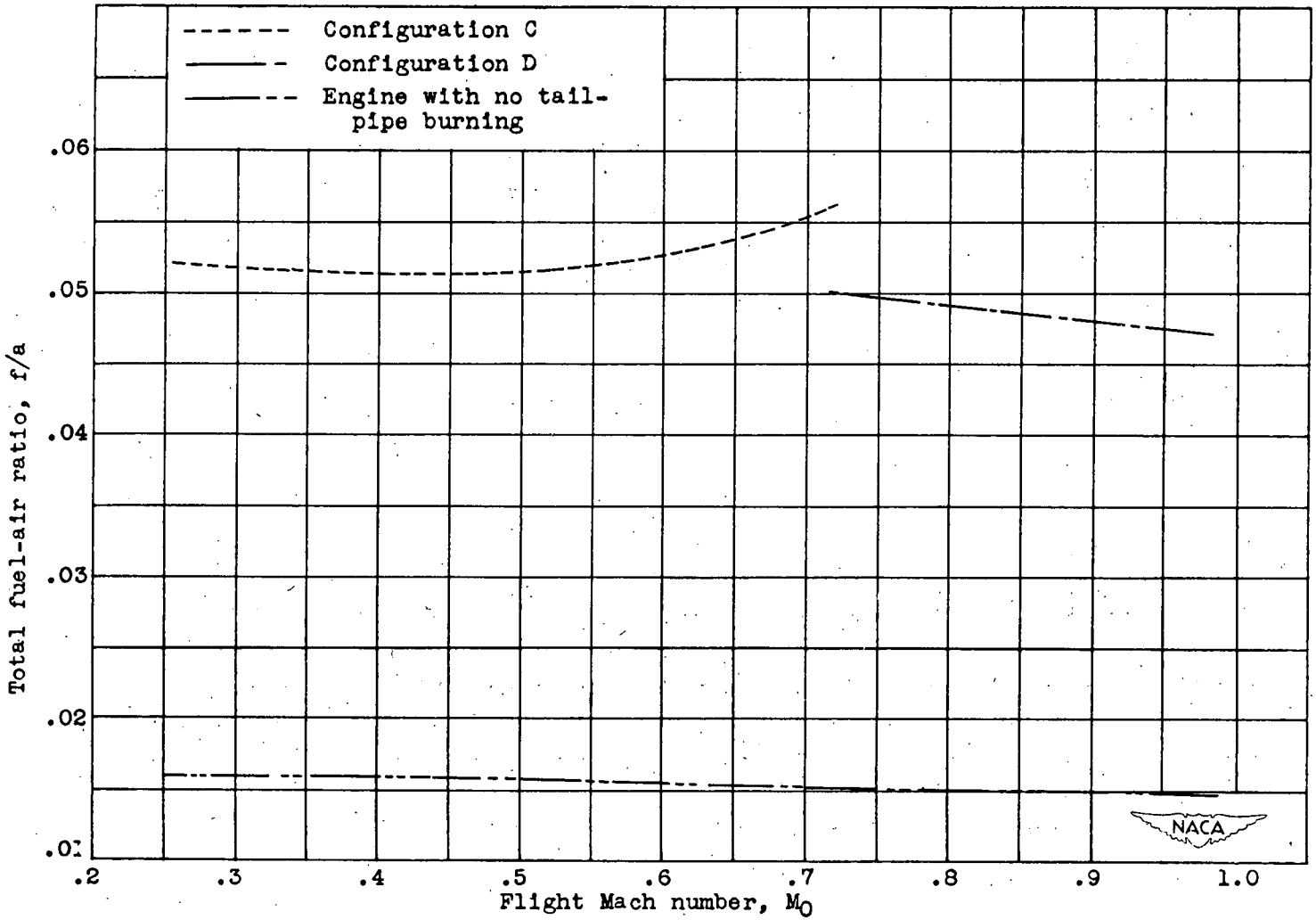

(b) Configurations C and D; modified engine; turbine-outlet temperature, T_6, 1650° R.

Figure 16. - Concluded. Relation between total fuel-air ratio and flight Mach number with standard tail pipe and with modified tail pipe and tail-pipe burning. Altitude, 25,000 feet; engine speed, 12,500 rpm.